



Review

# A Review of Advances in Graphene Quantum Dots: From Preparation and Modification Methods to Application

Yibo Cui <sup>1</sup>, Luoyi Liu <sup>1</sup>, Mengna Shi <sup>1,2</sup>, Yuhao Wang <sup>3</sup>, Xiaokai Meng <sup>4</sup>, Yanjun Chen <sup>2</sup>, Que Huang <sup>1,2,5,\*</sup> and Changcheng Liu <sup>1,2,\*</sup>

- <sup>1</sup> School of Environment and Safety Engineering, North University of China, Taiyuan 030051, China; 2114024330@st.nuc.edu.cn (Y.C.); 2214014114@st.nuc.edu.cn (L.L.); s202214039@st.nuc.edu.cn (M.S.)
- <sup>2</sup> Institute of Advanced Energy Materials and Systems, North University of China, Taiyuan 030051, China; yjchen@nuc.edu.cn
- <sup>3</sup> Hefei National Laboratory for Physical Sciences at the Microscale and Department of Chemistry, University of Science and Technology of China, Hefei 230026, China; sa22234082@mail.ustc.edu.cn
- <sup>4</sup> State Grid Shanxi Electric Power Research Institute, Taiyuan 030001, China; mengxiaokai870618@163.com
- <sup>5</sup> School of Resources and Safety Engineering, Central South University, Changsha 410010, China
- \* Correspondence: que.huang@nuc.edu.cn (Q.H.); ccliu@nuc.edu.cn (C.L.)

**Abstract:** Graphene quantum dot (GQD) is a new type of carbon nanometer material. In addition to the excellent properties of graphene, it is superior due to the quantum limit effect and edge effect. Because of its advantages such as water solution, strong fluorescent, small size, and low biological toxicity, it has important application potential in various fields, especially in sensors and biomedical areas, which are mainly used as optical electrical sensors as well as in biological imaging and tumor therapy. In addition, GQDs have very important characteristics, such as optical and electrical properties. There are many preparation methods, divided into top-down and bottom-up methods, which have different advantages and disadvantages, respectively. In addition, the modification methods include heterogeneous doping, surface heterogeneity, etc. There are still many challenges in developing GQDs. For example, the synthesis steps are still hard to conduct, but as the inquiry continues to deepen, GQDs will be revolutionary materials in the future. In this work, the literature concerning research progress on GQDs has been reviewed and summarized, while the key challenges of their application have been pointed out, which may bring new insights to the application of GQDs.

**Keywords:** heteroatomic doping; surface function; sensor; tumor treatment; biological imaging



**Citation:** Cui, Y.; Liu, L.; Shi, M.; Wang, Y.; Meng, X.; Chen, Y.; Huang, Q.; Liu, C. A Review of Advances in Graphene Quantum Dots: From Preparation and Modification Methods to Application. *C* **2024**, *10*, 7. <https://doi.org/10.3390/c10010007>

Academic Editors: Craig E. Banks and Aleksey A. Vedyagin

Received: 31 August 2023

Revised: 5 December 2023

Accepted: 25 December 2023

Published: 8 January 2024



**Copyright:** © 2024 by the authors. Licensee MDPI, Basel, Switzerland. This article is an open access article distributed under the terms and conditions of the Creative Commons Attribution (CC BY) license (<https://creativecommons.org/licenses/by/4.0/>).

## 1. Introduction

In recent years, with the development of science and technology and the enhancement of social awareness of environmental protection, the development and utilization of new energy sources and new materials have received attention from various countries [1]. Graphene, a new two-dimensional carbon material with  $sp^2$  hybridization, is the thinnest two-dimensional material ever discovered. Due to its properties of being very small and difficult to peel off the monolayer structure, even though scientists have carried out a lot of research, little has been achieved. In 2004, British researchers Andrei Geim and Kostia Novoselov succeeded in obtaining graphene from graphite by repeatedly folding special tapes [2], which won them the Nobel Prize in Physics in 2010. Since then, more and more research has been conducted on graphene, and many advantages of graphene have been gradually discovered, such as the fact that its strength is very large [3] and that it has a high transmittance [4]. Because of its many excellent optical, mechanical, and electrical properties, it is a revolutionary material with very important application potential in many fields.

Quantum dots, also known as “semiconductor nanocrystals”, are nanoscale semiconductors, generally spherical or spheroidal. Because these nanoparticles are very small, the quantum effect determines their characteristics. When UV light hits these semiconductor nanoparticles, they can emit various colors of light. Quantum dots have an important impact on modern life. Quantum dots used in LED display screens can make them have a wider color gamut and higher brightness; applied to the biological field, they can improve the imaging resolution of cells and tissues; and applied to the field of energy, they can greatly improve the efficiency of the battery. In the early 1980s, Louis Bruce and Alexei Yekimov each independently succeeded in synthesizing quantum dots. In 1993, Mungi Bavendi changed the method of making quantum dots to such a high quality that the trio were awarded the Nobel Prize in Chemistry in 2023, a technology that some say will bring about an energy revolution. Heiner Linke, a member of the Nobel Prize Committee for Chemistry and a member of the Royal Swedish Academy of Sciences, commented that quantum dots can be seen as a milestone in the whole field of nanotechnology and a huge breakthrough for mankind in regulating the properties of materials. Quantum dots have very important potential applications. In the field of quantum computing, they are expected to be used to prepare quantum bits. In the field of biology, they can be used for more accurate medical imaging, early cancer detection, and drug delivery systems. In other fields, they can be used to create highly sensitive sensors, for the development of more efficient lasers and photonics devices, and so on. In conclusion, quantum dots have now greatly affected people’s lives and are one of the high-profile technological revolutions. In the future, there will be more and more research.

The graphene quantum dots we are looking at are a combination of both. Quantum dots are semiconductor nanocrystals with a particle size generally less than 100 nm [5], characterized by a broad excitation spectrum and a long fluorescence lifetime. Graphene quantum dots are zero-dimensional graphene particles consisting of one or several layers of tiny graphene lamellae [6–8], so it is similar to graphene in crystal structure; it not only possesses various properties of graphene but also exhibits better performance due to the properties of quantum dot materials. First of all, we know very well that graphene has a zero band gap and does not produce luminescent behavior under light irradiation, which will greatly limit the range of applications of graphene materials in optics, whereas nanoscale GQDs have a band gap, and the existence of the band gap gives them the ability to produce electron holes [9], so GQDs are widely used in the optical industry instead of graphene. Secondly, GQDs have oxygen-containing groups represented by hydroxyl and carboxyl groups on the surface and edges of GQDs, which make GQDs possess better water solubility [10], and they can be chemically grafted by conjugated bonding. They can also be functionalized by doping heteroatoms or other materials to form composites, which expands the applications of GQDs. Finally, due to edge and quantum confinement effects, GQDs have the advantages of good biocompatibility, photobleaching resistance, chemical inertia, excellent optical properties, and high dispersibility [11–13].

Due to the good conductivity, photoluminescence ability, and fluorescence properties of graphene quantum dots, it can be used as a probe to identify various targets and has become a new research material in the field of sensing [14]. For example, in gas sensors, conductive polymers such as polyaniline, polythiophene, and their derivatives have been widely investigated as sensitive materials for gas sensors in previous studies because they can operate at room temperature and have excellent mechanical properties [15]. However, it was found to have poor thermal stability, which affects the application of polymer-based sensors. It was found that quantum dot materials have better specific surface area and unique surface effects, and their photoelectric properties are highly stimulus-responsive to gas adsorbents. Due to this property, GQDs have received increasing attention as gas-sensitive materials [16]. In addition, GQDs do not have significant toxicity compared to other conventional semiconductors [17], and GQDs have the advantages of being environmentally friendly and biocompatible, which allows them to be used in bioassays. Secondly, optical oxygen production and other characteristics can be used to treat cancer, etc., and

also have good application effects in biomedical fields [18]. However, in the process of synthesizing GQDs, a large number of other oxygen-containing groups will be produced, which can easily become the electron hole to non-radiation recombination center, thereby limiting its application in sensing and biomedicine, so we can modify graphene quantum dots to make their performance superior.

The main purpose of this paper is to introduce the current research status of GQDs, including the structure and properties of graphene quantum dots, their preparation and modification methods, and then introduce the research of graphene quantum dot composites in biomedicine, chemical sensing, and other related fields, as well as briefly summarize the challenges that they are currently facing, and finally look forward to the future direction of graphene quantum dot research.

## 2. Structure and Properties of Graphene Quantum Dots

### 2.1. Structure of Graphene Quantum Dots

Carbon nanomaterials can be categorized into zero-dimensional, one-dimensional, and two-dimensional carbon nanomaterials according to their dimensionality. Zero-dimensional carbon nanomaterials refer to carbon materials that are all nanoscale in three dimensions. There are mainly fullerene and fullerene-like  $C_n$ -structured carbon nanomaterials, nanodiamonds, carbon nanodots, and graphene quantum dots, which have different structures. In fullerenes, C atoms are hybridized into bonds with  $sp^2$ , a single carbon atom has a coordination number of 3, forming 3  $\sigma$  bonds with the surrounding three carbon atoms, and the remaining orbital forms a cloud of  $\pi$  electrons, thus forming aromatic carbon molecules [19]. Different from the  $sp^2$  hybrid bonding of fullerene and  $C_n$  structures, nanodiamonds is generally  $sp^3$  bonded inside, maintaining the integrity of the crystal structure as a whole, and there are graphite shells or carbon suspension bonds outside. Similar to nanodiamonds, carbon quantum dots are roughly spherical particles with internal carbon nuclei that maintain crystalline integrity, but the particle size of carbon quantum dots is smaller compared to nanodiamonds, typically around 10 nm.

Graphene quantum dots (GQDs) are a quasi-zero-dimensional form of graphene with the same crystal structure as graphene. The ideal infinite graphene crystal consists of two sets of nested sublattices (lattices A and B) with a distance of 0.142 nm between neighboring cells. and they belong to different sublattices, with three x-bonds inside each lattice and carbon atoms C occupying lattice points to form a periodic six-membered ring structure in the graphene plane [20]. C atoms are closely stacked, each carbon atom is connected to 3 carbon atoms by  $sp^2$ , 3 of the 4 valence electrons are paired with the valence electrons of the surrounding 3 carbon atoms to form  $\delta$ -bonds, and the unpaired  $\pi$ -electrons work together to form large  $\pi$ -bonds, and this unique electronic structure confers an allotropic nature that is different from that of other carbons. The structure of the graphene quantum dot is shown in Figure 1.

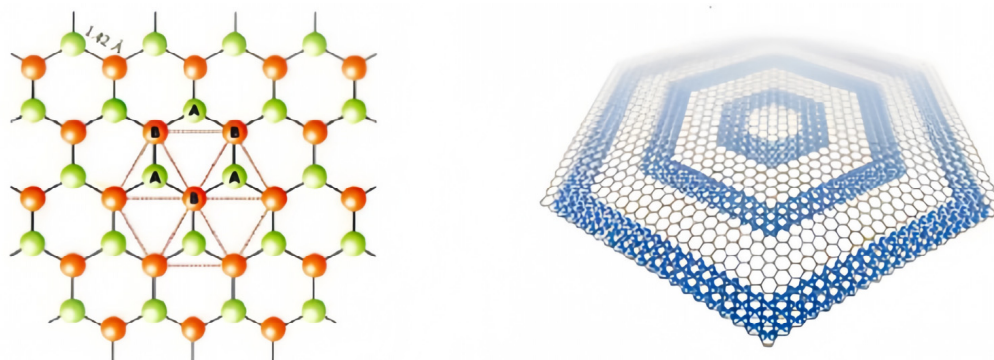


**Figure 1.** The structure of the GQDs.

## 2.2. Nature of Graphene Quantum Dots

### 2.2.1. Optical Performance

Graphene quantum dots have excellent photostability and photoluminescence properties, and their light-absorbing capacity is generally closely related to the structure of graphene oxygen-containing groups and quantum dots. They are usually reflective in the ultraviolet region, which decreases with increasing wavelengths [21,22]. The causes of light mainly include two aspects: the surface edge state and the conjugate  $\pi$  bond. The effects of surface edge states on the photoluminescence of graphene quantum dots include their jagged edge types, oxygen-containing groups, amino groups, and quantum dot nuclei. When graphene quantum dots only have fewer surface chemical groups, the band gap of conjugated  $\pi$  bonds is considered to be the main cause of photoluminescence, and the photoluminescence of graphene quantum dots can be adjusted by adjusting the size of the conjugated  $\pi$  bonds. Studies have found that GQDS has a long luminous wavelength and low energy. Compared with carbon quantum dots, there is a higher PL quantum yield. Zhu et al. [23] synthesized GQD with different fluorescences, which can range from the UV to the red light region and have better photostability than conventional fluorescent moieties. Li et al. [24] found that carbon quantum dots obtained by the alkali-assisted electrochemical method have good transition luminescence properties, excitation with a long wavelet length, and low energy. It has an important potential for applications in bioimaging and medicine.

### 2.2.2. Water Solubility

The surface of GQDs is rich in oxygen-containing functional groups, such as hydroxyl and carboxyl groups. Therefore, it is particularly water-soluble and can form a stable aqueous solution. In addition, some groups can be introduced on the surface of GQDs to change the types of hydrophilic and hydrophobic groups and synthesize many different graphene quantum dots. Cho et al. [25] coupled the synthesized hydrophilic GQD with  $N,N'$ -dicyclohexyl carbon diimide and reacted with epoxy ring-opening simultaneously, realizing the change of hydrophilic to hydrophobic GQDs.

### 2.2.3. Electrical Properties

(ECL) electrochemiluminescence is a luminescent phenomenon produced by electrochemical reactions in solution. As an analytical technique, ECL combines the advantages of chemiluminescence analysis without background light signals and reaction electrochemical analysis utilizing electrode potentials that are easy to control with the advantages of high sensitivity, good selectivity, and no acoustic noise. It should have outstanding advantages, such as a wide range. In recent years, many researchers have found that semiconductor quantum dots have ECL properties, while GQDs have a higher specific surface area and richer surface states and therefore have better potential as ECL luminophores [26]. Typically, GQD nanosheets, especially monolayer GQDs, have a higher specific surface area than CQD nanoparticles, which means that GQDs may have richer surface states. In addition, oxidized GQDs increase the emission sites of GQDs due to the increase of oxygen-containing functional groups, resulting in stronger electrochemiluminescence effects. For example, the hydrothermal onset potential of GQDs prepared from graphene oxide sheets can be as low as 0.4 V, and a stable ECL signal with a relative standard deviation of only 1.0% was measured in a continuous cyclic scan. Jung et al. assembled GO nanoplates into a porous network using an ion-mediated assembly (IMA) method. The metal substrate was immersed in GO solution, and GO nanosheets were attracted to the anode and adhered to the surface with the assistance of an applied voltage. The GO was then converted to reduced graphene oxide (rGO). Conductive rGO filters with a porous structure and a high specific surface area can be connected to voltage applications for novel electrostatic PM filtration. Ionic liquids (ILs) are liquids composed entirely of ions and have been widely studied in the field of electrochemistry due to their high conductivity and electrochemical stability [27].

#### 2.2.4. Toxicity and Cytocompatibility

Carbon is a vital element of human tissue and is non-toxic. In addition, a series of carbon-based compounds are the basis of human tissues. And the carbon material is chemically inert, so GQDs have excellent biocompatibility and environmentally friendly properties. Chong [28] et al. studied the toxicity of graphene quantum dots in organisms and in vitro in detail. In vitro experiments found that graphene quantum dots have extremely low toxicity due to their ultra-small size and high oxygen content, while in vivo experiments on the distribution of graphene quantum dots in mice showed that graphene quantum dots do not accumulate in the major organs of the mice but are rapidly excreted through the kidneys and do not show significant toxicity at high doses. Some researchers have demonstrated the very low cytotoxicity of graphene quantum dots by co-culturing graphene quantum dots with MC<sub>3</sub>T<sub>3</sub> cells and conducting MTT assay experiments. In conclusion, graphene quantum dots have very low cytotoxicity and good biocompatibility and can be used for high-concentration bioimaging and other biomedical applications. The effect of functional groups on the cytotoxicity of graphene quantum dots was determined by comparing their ability to produce reactive oxygen species. It has been shown that the keto carbonyl group has a significant effect on the reactive oxygen species formation ability of graphene quantum dots, so the removal of oxygen functional groups from graphene quantum dots improves the photostability and reduces the cytotoxicity of graphene quantum dots, which provides a molecular-level indication for better design of biocompatible graphene quantum dots. Graphene quantum dots with a large number of oxygen-containing groups are effectively used as surgical nanoradiation sensitizers for radiation therapy due to their good biocompatibility [29]. The results show that GQDs have very high biocompatibility and low in vivo cytotoxicity compared to quantum dots [30].

### 3. Preparation of Graphene Quantum Dots

There are many methods for the preparation of graphene quantum dots, and the synthesis can include the “top-down method” and the “bottom-up method” [22]. The top-down strategy focuses on the use of chemical, electrochemical, or physical means to cut large areas of graphene oxide, carbon nanotubes, carbon fibers, and carbon black, which contain a large amount of graphene structure, to form GQDs of very small size [31]. Such methods mainly include microwave ultrasound-assisted peeling, chemical peeling, the hydrothermal method, the solvothermal method, and the electrochemical peeling method [32]. For example, Li [33] et al. prepared quantum dots by laser ablation; Zhang [34] et al. prepared graphene quantum dots by pyrolysis; and Wang [35] et al. used ultrasonic-assisted chemical oxidation to prepare yellow visible fluorescent carbon quantum dots from petroleum coke. The advantages and disadvantages of each method from top to bottom are listed in Table 1.

**Table 1.** The advantages and disadvantages of each method, from top to bottom method.

	Methods	Advantages	Disadvantages	Refs.
Top-down	Hydrothermal synthesis; Solvothermal synthesis	Large output; Simple operation	Irregularly size and shape; Strong reductants are needed	[24,36,37]
	Acidic oxidation	Large output; Simple operation	There are lots of oxygen-containing functional groups left on the GQD surface; Numerous defects	[38]
	Oxidation cutting	Relatively cheap raw materials; Large output; Simple operation	Too much oxygen—containing functional groups	[39]
	Ultrasonic exfoliation	Simple operation; No reduction process; Fewer surface defects and more stable electronic properties	Depending on the quality of the carbon fiber, Special devices are needed	[39–41]

There are many advantages to the top-down method, namely that raw materials are easy to obtain, easy to operate, have a large output, and have a relatively simple process flow. However, the disadvantages are also very obvious. Firstly, it is difficult to remove the by-products in the GQDs prepared by the chemical cutting method, and secondly, it is difficult to precisely control the structure and size of the GQDs when doing the experiments due to the randomness of the cutting sites and the large proportion of defects in the products, and thus the quantum yield is often not high. The bottom-up strategy mainly uses small-molecule carbon-containing compounds (such as citric acid, glucose, pyrene, etc.) as carbon source materials and directly prepares graphene quantum dots through chemical means to control the reaction. Such methods mainly include metal catalysis, pyrolysis carbonization, the soft template method, solution chemistry, etc. [9]. For example, Lu [42] et al. successfully prepared GQDs with a fixed structure by controlling the heating temperature using the fullerene open-cage method. The advantages of this method are that the size and morphology of graphene quantum dots can be adjusted very accurately, and the quantum yield ratio is also high. The disadvantage is that the operation steps are cumbersome and complicated.

The advantages and disadvantages of each method, from bottom to top, are listed in Table 2.

**Table 2.** The advantages and disadvantages of each method, from bottom to top method.

	Methods	Advantages	Disadvantages	Refs.
Down-top	Carbonization of organic molecules	Well-defined, monodispersed structures; Simple operation	Low-output	[43,44]
	C <sub>60</sub> open cage method	Well-defined monodispersed structures; Precise control over both size and shape	Strict reaction conditions; Very high heating temperature; Expensive raw materials	[44]
	Solution chemical method	Well-defined monodispersed structures; Easy control of both size and shape; High purity	Difficulty preventing aggregation; Low-output	[44,45]

### 3.1. Top-Down Method

#### 3.1.1. Electrochemical Method

The electrochemical method mainly uses graphite and carbon fibers as anode materials to provide carbon sources and uses the defects in graphite as sites for electrochemical oxidation to drive free radicals in solution to cut the carbon source materials under the action of an applied electric field to produce hydroxyl, carboxyl, and other oxygen-containing functional groups. At the same time, the ions generated by the electrolyte act as electrochemical scissors under the action of the electric field force to cut the graphene flakes into small and intact GQD structures by oxidizing the C-C bonds. Huang et al. [46] used graphene paper as an anode and ammonia water as the electrolyte to prepare amino-functionalized GQDs with an average diameter of 4.7 nm. Tan et al. [47] successfully prepared graphene quantum dots using graphite rods as carbon source material and potassium persulfate aqueous solution as an electrolyte. Li et al. [24] prepared GQDs in a phosphate buffer solution using graphene film as an electrode, and their properties were very stable. Wongrat et al. [48] used graphite rod as carbon source material and citric acid and KCl as mixed electrolytes to peel graphite into GQDs with an average diameter of 2.6 nm. Various research results have shown that the yield of GQDs prepared by weak electrolytes is much higher than that of strong electrolytes. This is mainly due to the fact that a strong electrolyte will prematurely tear the graphene paper and detach it from the anode, which in turn stops the electrochemical cutting. The preparation method of the electrochemical method is shown in Figure 2. This method can obtain GQDs with stable quality, but the raw material processing is complex and the yield is low, so it is difficult to prepare on a large scale.

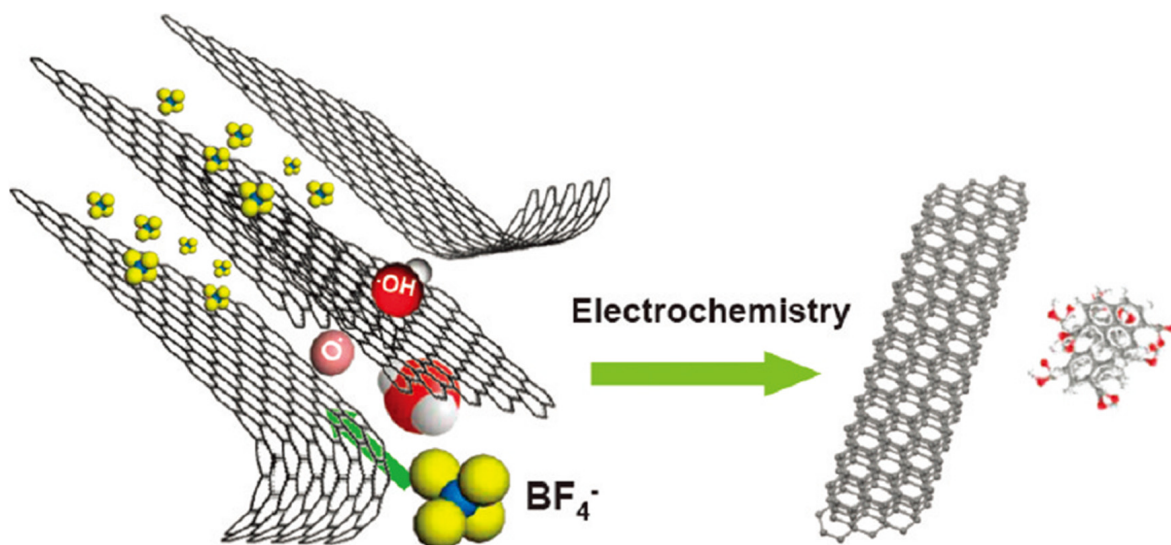


**Figure 2.** Electrochemical preparation GQDs [32].

### 3.1.2. Hydrothermal Method and Solvothermal Method

The principles of the hydrothermal method and the solvothermal method are basically similar; compared to other types of synthesis methods, this method is a relatively simplified one. The mechanism of the hydrothermal method is to oxidize the carbon source material, generate a large number of oxygen-containing functional groups on its surface, further oxidize to carbonyl pairs at room temperature, and then add NaOH,  $\text{NH}_3 \cdot \text{H}_2\text{O}$ , and other alkaline substances. Due to the instability of carbonyl pairs, carbon atoms on epoxy bonds can be removed under the action of hydrothermal action, thereby breaking up to obtain GQDs. The method is mainly divided into three stages: (1) oxidation of graphene in a mixture of concentrated sulfuric acid and concentrated nitric acid; (2) oxygen-containing functional groups such as epoxy groups are introduced on the oxidized graphene sheet, and these oxygen-containing functional groups tend to be arranged in a straight line on the carbon skeleton; (3) the oxidized graphene is subjected to hydrothermal treatment under weak alkaline ( $\text{pH} = 8$ ) conditions to remove oxygen-containing groups, resulting in sheet rupture, the formation of GQDs, and finally filtration and purification. The main difference between the solvothermal method and the hydrothermal method is that DMF and other organic solvents with certain reducing properties are used instead of water as solvents, and graphene is reduced while being broken. Su et al. [49] prepared nitrogen-doped graphene quantum dots (N-GQDs) by the one-step hydrothermal method using graphene oxide, ethylenediamine, and hydrogen peroxide as raw materials. Pan et al. [36] obtained GQDs with a size of 5–13 nm by using a three-step hydrothermal method. He used graphene oxide and concentrated acid as raw materials for the reaction under alkaline conditions. According to the reaction mechanism, there may be some mixed epoxy chains in the graphene oxide sheets, which are composed of fewer epoxy groups and more carbonyl groups, and the presence of these linear defects makes the GSs susceptible to attack and fragmentation. Because tricarbonylenes are most common at jagged edges, the two electronic leaps observed in PL spectra can be viewed as leaps from the  $\sigma$  and  $\pi$  orbitals to the lowest unoccupied molecular orbital. A hydrothermal method was developed to cut pre-oxidized GSs into ultrafine GQDs with strong blue-light emission. The discovery of new PLs bands from GQDs will extend the applications of GQDs materials in other fields such as optoelectronics and biological labeling [50]. Pan et al. [51] and Li et al. [50] improved the three-step hydrothermal method, respectively, and Pan et al. [51] changed the weak alkaline condition of the hydrothermal condition to a strong alkaline  $\text{pH} > 12$ , which reduced the product size to 1.5–5 nm. The preparation method is shown in Figure 3. Li et al. [50] modified the surface passivation of the product GQDs with PEG to increase

the fluorescence quantum yield to 28%. Shen et al. [52] first used hydrazine hydrate to reduce GO after the surface was passivated by PEG to prepare GQDs, and then restored it by the hydrothermal method after improvement. Compared with Pan et al. [51], the main difference was that the surface of GQDs was passivated by PEG. Xie et al. [53] used different carbon materials as carbon sources, such as carbon nanotubes (CNTs), graphene oxide (GO), and carbon black (CB), and prepared GQDs by hydrothermal method (products were expressed as C-GQDs, G-GQDs, and S-GQDs, respectively). The main reaction mechanism of this method is that, during the reaction process, the oxidant  $H_2O_2$  used is generated under hydrothermal conditions. OH, these free radicals can make more efficient oxidative cleavage of carbon materials at high temperatures. The results show that the prepared C-GQDs have a uniform size distribution and the smallest particle size, while the PL fluorescence intensity order of the obtained GODs is exactly the opposite, with C-GQDs being the largest and S-GQDs being the smallest, and the fluorescence intensities of C-GQDs are 1.3 times and 1.5 times that of G-GQDs and S-GQDs, respectively. Further studies showed that the particle size of the three GQDs tended to gradually decrease with an increase in reaction temperature. PL spectroscopic studies have shown that the PL spectrum of GQDs is blueshifted as the particle size decreases. This study provides a method that can effectively adjust the fluorescence properties of GQDs, so it is expected to be well applied in the fields of optoelectronic devices and biological imaging.

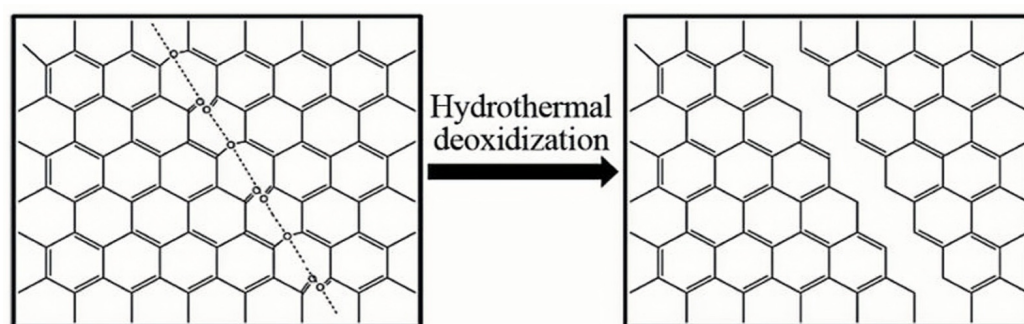


**Figure 3.** Effect of hydrothermal deoxidization [36].

### 3.1.3. Chemical Stripping Method

The chemical stripping method can also be referred to as strong acid oxidation or oxidative cutting. The working principle is to use the oxidizing effect of strong acids and strong oxidizing agents to directly cut carbon materials such as graphene oxide and carbon nanotubes to obtain nanoscale GQDs [38]. Influenced by its own functional groups, the carbon material has a tendency to fracture in a jagged direction in the microstructure, so it can be cleaved to form GQDs by chemical oxidation. The most important feature of this method is that by controlling the temperature in the reaction, GQDs of different sizes and emitting different colors of fluorescence can be obtained. For example, GQDs emitting blue, green, and yellow fluorescence can be prepared at 120 °C, 100 °C, and 80 °C, respectively. The method is simple and effective and is suitable for the large-scale production of GQDs, but it requires the use of strong acids, such as sulfuric or nitric acid, in the preparation process. However, this method introduces other oxygen-containing groups, which leads to increased toxicity of GQDs, and it is difficult to remove the oxidant used in the oxidation process, which seriously affects the biocompatibility of the product GQDs. Peng [38] et al. used a very simple method, as shown in Figure 4, to prepare GQDs by stripping carbon fiber with a mixture of concentrated sulfuric acid and concentrated nitric acid. By controlling the temperature, GQDs with different emission colors and sizes were obtained, which could be used as fluorescent biological probes. With the deepening of research, people gradually began to look for green oxidants to replace strong acids and made certain progress. For example, Lu et al. [54] used black carbon as a precursor and  $H_2O_2$  as an oxidant to produce graphene quantum dots, and the only products that came out of the reaction were  $H_2O$  and GQDs, which not only avoided the intrusion of other impurities but also did not require

other subsequent steps, and the synthesized graphene quantum dots were uniform in size with good photostability and biocompatibility. The produced GQDs can be well applied as fluorescent probes for biological cell imaging, which is the fastest green preparation method reported so far compared with other reported research methods and provides a new idea for the green preparation of GQDs.

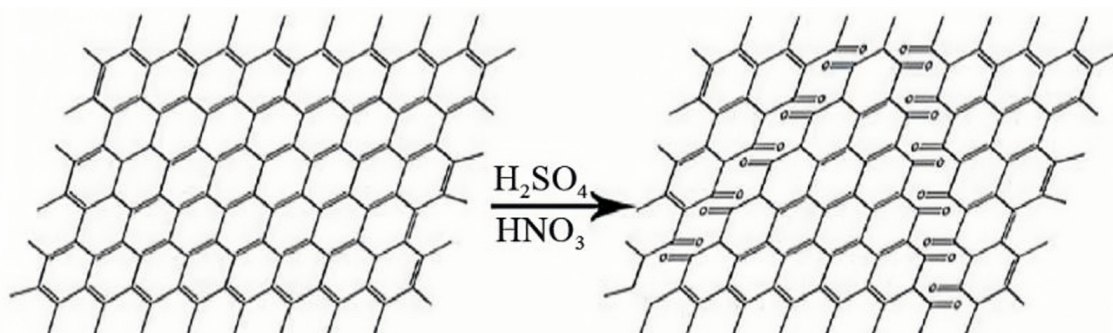


**Figure 4.** Chemical stripping method [38].

#### 3.1.4. Microwave Ultrasonic Assisted Stripping Method

General top-down strategy methods such as hydrothermal and electrochemical methods are not suitable for large-scale production of GQDs due to the large reaction time required for heating by conventional heating sources. Thus, we can utilize microwave radiation to provide additional heat, which can significantly shorten the reaction time, resulting in the rapid formation of high-quality GQDs. In addition to microwave-assisted stripping, ultrasound-assisted stripping has also been used for the simple and gentle fabrication of GQDs. The basic mechanism is that ultrasonic waves will produce alternating high and low pressure waves in the liquid, which will continuously form vacuum vacuoles, and under the action of pressure, the vacuoles gradually rupture. They produce high-velocity liquid jets and strong hydrodynamic shear forces to shear the material together. Li et al. [39] reported for the first time the preparation of GQDs by microwave-assisted chemical cracking of GO tablets under acidic conditions. The preparation method is shown in Figure 5 and tested the ORR performance of graphene composite materials. This method not only shortens the reaction time but also increases the quantum yield of graphene quantum dots. The mechanism is initiated by the acid oxidation of epoxy groups, which forms hybrid lines on some specific types of carbon lattices, making them vulnerable to attack. With the advantages of low cytotoxicity, low cost, and easy labeling, such ECL-active GQDs are expected to have a promising application in the development of novel ECL biosensors [55]. Luo et al. [40] reported the two-step preparation of white fluorescent GQDs. Methods: Yellow-green fluorescent GQDs were pre-synthesized under ultrasonic and microwave irradiation. The average transverse size of GQDs was more uniform. After irradiation with microwaves in an alkaline environment, the GQDs were converted into WGQDs, which were photochemically stable and non-toxic. According to the test results, the lateral sizes of WGQDs remained at similar intervals and were also more uniform. Measurements with atomic force microscopy (AFM) showed that the prepared graphene quantum dots consisted of multilayer graphene. Zhuo et al. [41] first prepared GQDs from graphene by direct ultrasonic spalling. Tang et al. [45] used glucose as a precursor to prepare GQDs of uniform size by using the glucose microwave-assisted hydrothermal method (MAH). Due to the microwave assistance, the resulting product has a good size and appearance, and because the only reactant in the reaction process is glucose, no surface passivator or inorganic additives are required, so the purity of the product GQDs is high.

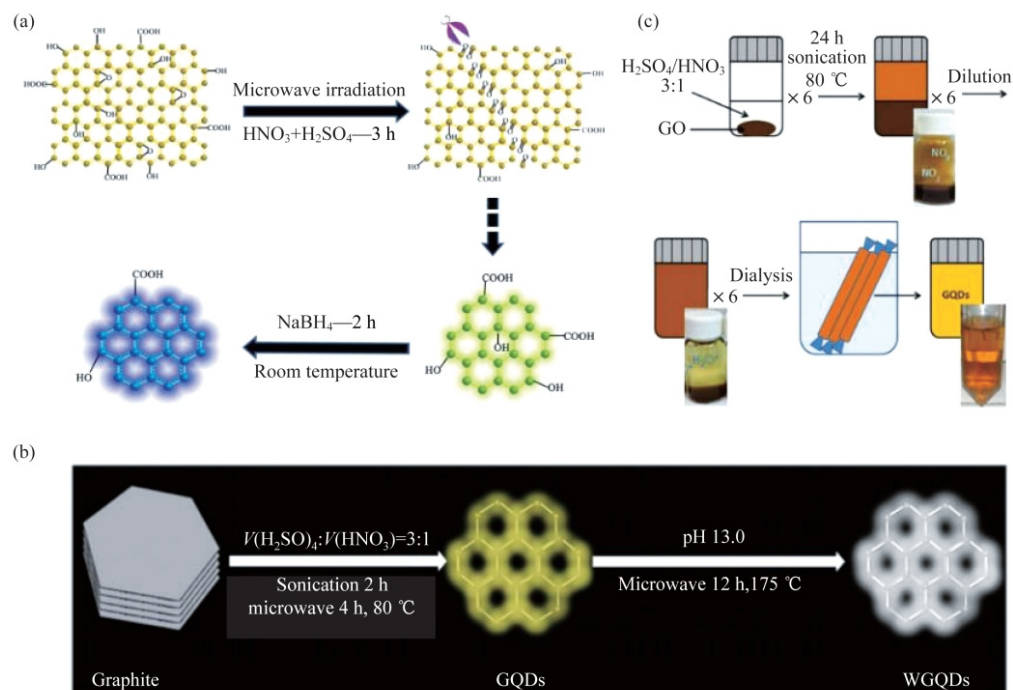


**Figure 5.** Microwave/Ultrasonic Dipping Method Diagram (a): Prepare GQDs through the chemical cracking of the microwave-assisted GO tablet; (b): WGQDs preparation process; (c) Mixed acid stripping GO preparation GQDs [39].

### 3.2. Bottom-Up Method

#### 3.2.1. Carbonization and Pyrolysis Method

The carbonization pyrolysis method can also be called the small-molecule carbonization method, which has become a very simple method due to the continuous research on GQDs. The basic mechanism is to use an instrument to heat the small-molecule precursor carbon source material at a temperature higher than its melting point, and when it reaches a certain temperature, it condenses and condenses to obtain a small-molecule graphene quantum dot material. This method can use many different precursors, such as ethanolamine, amino acids, coffee grounds, carbohydrates (sucrose or glucose), citric acid, etc. [43], and different precursors can produce different types of GQDs. The carbonized thermal solution method of using glucose as a carbon source is shown in Figure 6. Precursor molecules for the preparation of pyrolysis-mediated GQDs generally include both aromatic and non-aromatic moieties; the former can be directly pyrolyzed to obtain the materials due to the presence of off-domain orbitals, but the non-aromatic moieties have to undergo intramolecular and intermolecular dehydrogenation for the preparation of GQDs. Shehab [56] et al. directly carbonized glucose at high temperature to obtain water-soluble GQDs, which have a size of 7~10 nm, high crystallinity, and a large number of carboxyl groups at the edge. Qu et al. [57] prepared N- and S-co-doped GQDs using thiourea and citric acid as precursors, respectively. Liu et al. [58] used hexaphenylbenzene as a carbon source to prepare uniform-size GQDs; their transverse size is 60 nm and their longitudinal thickness is 2~3 nm. Its basic process is mainly divided into three steps: first, the use of dehydrogenation cyclization will result in six Phenylbenzene becoming powder, and then artificial graphite is obtained by carbonization cracking. Finally, GQDs were prepared using artificial graphite as a carbon source and recovered with hydrazine, originally to increase their quantum yield [58].

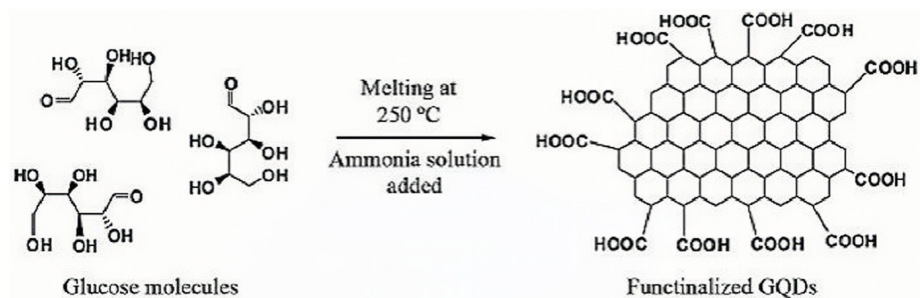


**Figure 6.** Citric acid as a carbon source in the carbonized thermal solution method [56].

### 3.2.2. C<sub>60</sub> Open Cage Method

The basic mechanism of preparing graphene quantum dots by the C<sub>60</sub> open-cage method is to prepare GQDs with homogeneous morphology by controlling the temperature and using a mixture of active transition metals or a mixed solution of strong acids and strong oxidizers to open the fullerene under certain reaction conditions. The main reaction process is as follows: when the temperature is heated to a certain degree, due to the different lattice constants of C<sub>60</sub> and Ru single crystals, under the catalytic effect of the transition metal Ru, the carbon atoms in the C<sub>60</sub> molecules will be embedded in the surface of Ru single crystals and will be gradually fractured into carbon clusters; and then, when annealed at different temperatures, these clusters will undergo diffusion and aggregation to form different shapes and sizes of GQDs, and the shapes and sizes of GQDs can be controlled by changing the annealing temperatures and densities of clusters. Loh et al. [42] reported the catalytic decomposition of fullerenes (C<sub>60</sub>) by the live-wave transition metal Ruthenium (Ru) to prepare a series of atomic-level GQDs. Lu et al. [42] used ruthenium metal to catalyze the fracture of C<sub>60</sub> to generate carbon clusters under high temperature conditions, which were then diffused and aggregated to obtain GQDs. Lu [42] prepared GQDs of different sizes and morphologies by adjusting the temperature by the cage opening method, which proved the advantages of such methods. The mechanism chart for C<sub>60</sub> to prepare GQDs is shown in Figure 7. Kaciulis et al. [59] mixed fullerenes, H<sub>2</sub>SO<sub>4</sub>, and NaNO<sub>3</sub> in an ice water bath, then added KMnO<sub>4</sub> for reaction and dialysis to obtain GQDs with a transverse size of about 15 nm and a thickness of about 0.5–2 nm.

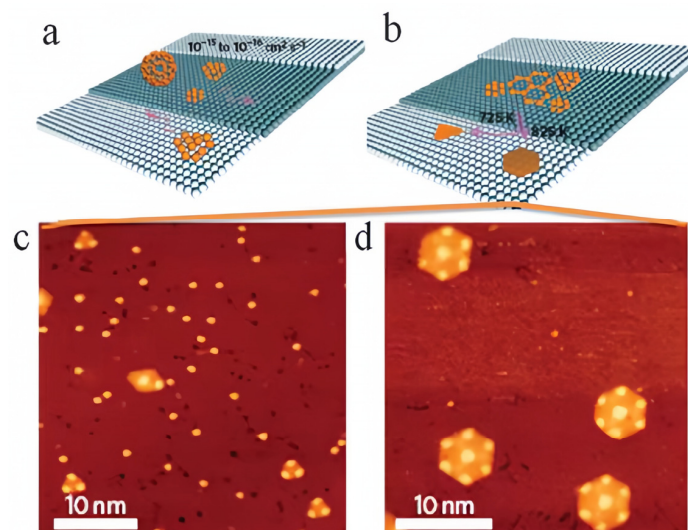


**Figure 7.** (a) Most C<sub>60</sub> molecules are adsorbed on the class and decompose the carbon clusters that produce limited mobility; (b) GQDS that is scattered on the surface of the surface to form different appearances that depend on the temperature of the annealing temperature; The appearance is (c) a triangular GQDS and (d) the STM image corresponding to the hexagonal GQDs with the tunnel parameters:  $v = 0.5 \text{ V}$ ,  $i = 1 \text{ na}$  [42].

### 3.2.3. Solution Chemical Method

Solution chemistry is also a more commonly used method in bottom-up strategies, and GQDs are formed after continuous oxidation and polymerization of small molecules. However, this method has a drawback: as the size of the polymer continues to increase, the gravitational force between the bonds increases, and the water solubility of the formed product will become lower and lower, so we generally need to adopt the solubilization method, that is, connect the solubilization group at the edge of the GQDs, so that the reaction can be carried out better. Li et al. [44] based their study on the oxidative condensation reaction using small organic molecules as precursors. By precisely controlling the ring number of six rings of graphene quantum dots, quantum dots with different ring numbers are obtained, and the precise control of GQD size is realized. The GQDs prepared by this method have a precise molecular structure, and the band gap or other properties of the GQDs can be further adjusted by adjusting the size of the GQDs or modifying other functional groups on their molecules. Although this method can precisely design and control the molecular structure and size of GQDs, the process is particularly complicated due to the multi-step organic synthesis reaction involved in the preparation, and the yield of GQDs is relatively low, so there are few research reports on the preparation of GQDs by this method.

### 3.2.4. Chemical Vapor Deposition Method

Chemical vapor deposition (CVD) is a common method for preparing 2D graphene. In CVD technology, the flow rate of hydrogen ( $H_2$ ) and C sources, growth time, temperature, and the surface morphology of the substrate are key parameters that determine the size of the final product. By adjusting these parameters, the nucleation rate of graphene can be accelerated to exceed the growth rate, thereby reducing the size of the final graphene product. The CVD method is commonly used to synthesize graphene, and rarely is CVD utilized to synthesize GQDs. Fan et al. [60] invented a chemical vapor deposition (CVD) reaction on a copper substrate to synthesize GQDs, with the advantages of fast synthesis speed, controllable quantum dot size, and good dispersion. Lee et al. [61] reported the use of the chemical vapor deposition (CVD) method to fabricate uniform GQDs by size control. The fabrication process was divided into two components: the first step required the assembly of PS-PDMS BCP films on raw materials, followed by the preparation of monolayer graphene on Si/SiO<sub>2</sub> substrates using chemical vapor deposition. The second step involves the use of ordered arrays of silicon dots generated by an oxygen plasma etching process as a mask layer for the patterning of the GQDs, which is important for improving the performance of the GQDs as well as for understanding the effects of size and functionalization on the GQDs.

The main methods currently used in research to synthesize graphene quantum dots are hydrothermal, chemical oxidation, and strong acid exfoliation, which have many advantages but have drawbacks that prevent them from being scaled up to the industrial quantities required for large-scale applications. So in the subsequent research on the continuous improvement of the production methods, Some researchers and scholars have now found some novel methods, and the microwave irradiation method mentioned above not only makes the reaction time much shorter but also can greatly improve the quantum yield. This method not only eliminates the need for additional reductants to avoid the introduction of impurities but also integrates the sheet-cutting and reduction processes. Environmentally friendly, green technology is also a requirement for our existing industries. In many methods studied so far, the synthesis of GQDs requires high-quality carbon precursors, toxic organic solvents, concentrated acid or alkali treatments, and high temperatures, which may produce a large number of impurities, and people have begun to look for new and environmentally friendly methods for their preparation. For example, in the preparation of GQDs from carbon-containing wastes, Wang et al. [62] used coffee grounds as raw material, Ding et al. [63] used renewable lignin as raw material, and Tran et al. [64] used gelatin as raw material, realizing the effective utilization of solid waste. A technique

applicable to the preparation of large-scale nonfunctional QDs has also been proposed, based on the principle that graphite suspensions are passed through micrometer-sized z-channels at high speeds and pressures to generate high shear rates, whereas millimeter-sized suspensions of graphite flakes are first exfoliated into micrometer-sized graphene, which is then further shrunken and fragmented into nanometer-sized QDs [65]. Methods of preparing graphene quantum dots are still being researched, and we may see more efficient and environmentally friendly methods in the future.

#### 4. Characterization of Structural Properties of Graphene Quantum Dots

We have summarized the preparation methods of graphene quantum dots in a more systematic way, but whether the structural properties of graphene quantum dots prepared by different methods change or not, in order to have a better in-depth understanding, we decided to choose the most promising method available—the hydrothermal method—to prepare graphene quantum dots and to characterize their structural properties.

Among the many methods for the preparation of graphene quantum dots, the hydrothermal method is one of the most commonly used due to its simplicity, the lack of special equipment, and the homogeneity of the synthesized products. Experimentally, blue fluorescent graphene quantum dots were synthesized by hydrothermal chemical reaction using micrometer-sized graphene sheets (GSs) as raw materials. Their TEM results are shown in Figure 8. Using the Gaussian function, the diameters of graphene quantum dots are mainly distributed between 5 and 13 nm, and their average particle size is 9.6 nm, which is a relatively narrow particle size distribution, indicating that the synthesized graphene quantum dots are relatively uniform in particle size [40].

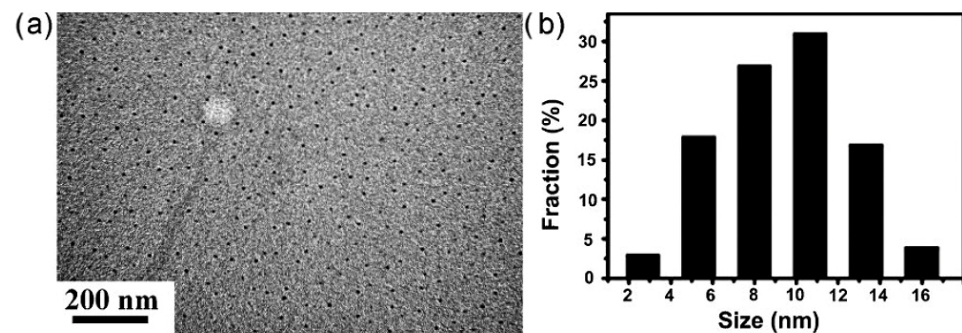


Figure 8. (a) TEM image of GQD; (b) GQD Size Distribution Chart [36].

The atomic force microscopy (AFM) analysis of graphene quantum dots is shown in Figure 9, which indicates that most of the graphene quantum dots have a thickness of about 1–2 nm, i.e., the quantum dots consist of two layers of graphene. The prepared graphene quantum dots have a size of 9.6 nm and a thickness of 1 nm, which means that our graphene quantum dots have a disk-like rather than spherical shape [40].

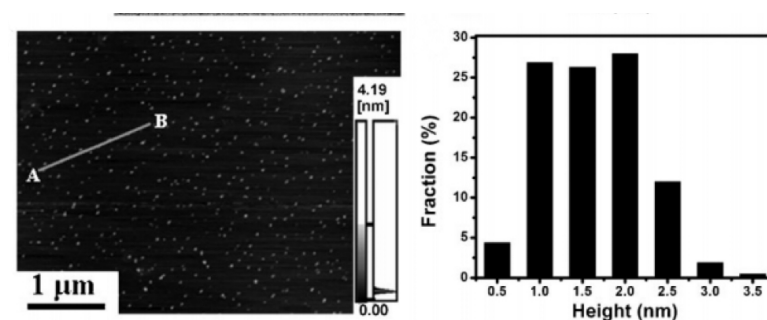
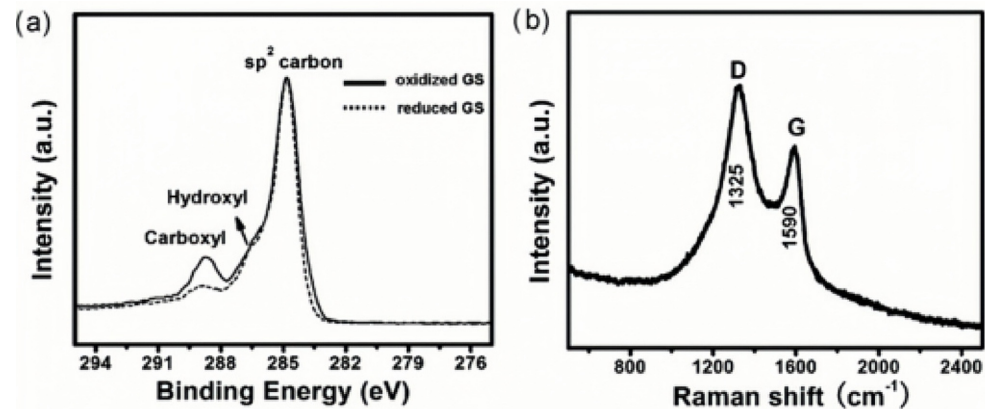


Figure 9. AFM image of GQD and height profile along the line A-B of GQD [36].

The compositions of the prepared graphene quantum dots were analyzed, and Figure 10a shows the full-scan XPS spectra of the oxidized and hydrothermally reduced GSs, and it can be clearly seen that the carboxylate signal at 289 eV is weakened after the hydrothermal treatment, while the  $sp^2$  carbon peak at 284.4 eV remains almost unchanged; and Figure 10b shows the Raman spectra of the reduced GSs of the graphene quantum dots, with one G-band at  $1590\text{ cm}^{-1}$  and a D-band at  $1325\text{ cm}^{-1}$  and they have an intensity ratio of 1.26 [40]. From the figure, there are very distinct and sharp absorption peaks, indicating that graphene quantum dots are mainly composed of C=C.



**Figure 10.** (a) XPS C1s spectra of the oxidized and hydrothermally reduced GSs (b) Raman spectra of the hydrothermally reduced GSs [36].

The fluorescence spectra of graphene quantum dot solutions at different excitation wavelengths were tested using a fluorescence spectrometer. The results are shown in Figure 11a. From the figure, it can be seen that at the excitation wavelengths from 320 to 410 nm, the position of the detected PL peak remained at 430 nm, and the PL peak was independent of the excitation wavelength. Meanwhile, with the increase in the excitation wavelength, the PL intensity is strong and then weak, and the luminous intensity is maximized at the excitation wavelength of 350 nm. With the gradual increase of the excitation wavelength, the PL peak was red-shifted with the increase of the excitation wavelength. Using quinine sulfate as a standard reference, the quantum yield of our prepared graphene quantum dots was calculated to be 6.9%. As can be seen from Figure 11b, the wavelength of the PL peak becomes larger under the excitation at 320–420 nm. Meanwhile, the concentration intensity gradually becomes weaker with the increase in the excitation wavelength.

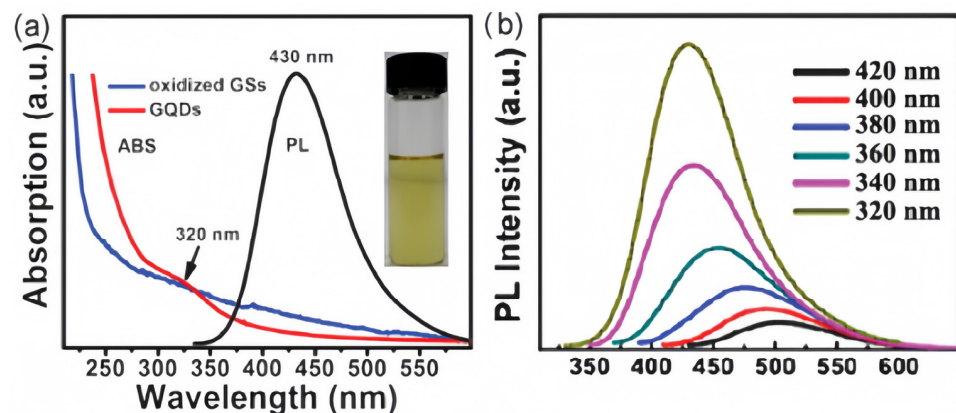


**Figure 11.** (a) UV-vis absorption (ABS, red) and PL (at 320 nm excitation) spectra of the GQDs dispersed in water; UV-vis absorption (ABS, blue) spectrum of oxidized GSs. Inset: Photograph of the GQD aqueous solution taken under visible light. (b) PL spectra of the GQDs at different excitation wavelengths [36].

The prepared graphene quantum dots were characterized by structural characterization, morphological characterization, and fluorescence properties, and the main characterization methods were TEM, AFM, and XPS. The results show that the prepared graphene quantum dots have abundant oxygen-containing functional groups, including carboxyl, hydroxyl, and carbonyl groups. The morphology of graphene quantum dots was characterized by TEM and AFM, and from the characterization results, we can see that the graphene quantum dots are more concentrated in terms of the size distribution and the thickness, which indicates that the graphene quantum dots are discoidal rather than columnar in shape, and that the graphene quantum dots have obvious lattice stripes, which indicates that the crystalline properties of the graphene quantum dots are good; they have good crystallization properties. For the characterization of fluorescence properties, most researchers believe that the absorption peaks between 200 and 270 nm are attributed to the C=C bond  $\pi$ - $\pi^*$  jump, while the absorption peaks larger than 260 nm are attributed to the C=O bond  $n$ - $\pi^*$  jump, while our graphene quantum dots have an absorption peak at 280 nm, which suggests that it is caused by the C=O of the graphene quantum dots, and the electron jump mode is  $n$ - $\pi^*$  jump [22]; The photoluminescence spectra of graphene quantum dots prepared by the hydrothermal method show that the fluorescence intensity of graphene quantum dots is different at different excitation wavelengths but exhibits the same law: with the increase of the excitation wavelength, its fluorescence intensity is stronger and then weaker, and there will be the maximum luminescence intensity at a certain wavelength of irradiation.

## 5. Modification Method of Graphene Quantum Dots

With the continuous research on graphene materials, a relatively complete set of preparation methods has been formed. However, in the process of research, people have continuously found that, in some aspects, ordinary graphene quantum dots are not very useful, while modified GQDs can play a great role. and the modification can not only improve the conjugation of the overall structure but also change its own fluorescence properties, biocompatibility, and other properties, which will enhance the quantum yield and optical properties of graphene quantum dots [39,66]. There have been many studies on the modification of graphene quantum dots, and the modification methods are generally categorized into three kinds: heteroatom doping, grafting modification, and constructing heterojunction.

### 5.1. Heteroatomic Doping

People have studied a lot about the doping of graphene quantum dots. Among them, the heterogeneous atoms are nitrogen [67], boron [68], sulfur [69], and some metal elements such as doping, as well as the methods of boron-nitrogen [70], nitrogen-phosphorus, etc. The chemical activity and electronic structure of GQDs doped with different atoms will be greatly improved, and their quantum yield will be increased. Doping different dopants will make different changes in their physicochemical properties, so it is important to choose different dopants according to the application [71]. The combination of doped metal elements with hetero-covalent bonds contributes to the improvement of electron transfer capacity [72,73]. However, the radius of general metal elements is large, and doping into carbon atoms may cause inhomogeneity, and some metals are also toxic, which may lead to ineffectiveness. Non-metallic ions can enter the semiconductor to form stable chemical bonds, so the study of non-metallic doping will be the main research direction.

#### 5.1.1. Nitrogen Doping

Nitrogen doping has become one of the most common and effective methods to modulate the quantum yield and improve the fluorescence performance of GQDs. Since nitrogen is adjacent to carbon in the chemical element table with a small difference in radius, its electronegativity is greater than that of carbon. The doped nitrogen will resonate with the effective orbitals of GQDs and improve the electronic activity, which makes it easier to be

doped into GQDs. It has been found that doping N atoms into the original nanomaterial enhances its PL behavior, leading to enhanced applications in biosensing, fluorescence imaging, and several other areas [65]. Common nitrogen sources generally include ammonia [74], dimethylformamide (DMF), nitric acid [74], melamine, and quadrol [75]. A diagram of a laser ablation device is shown in Figure 12. Calabro et al. [75] synthesized N-GQDs based on a variety of substances in ammonia, quadrol, and pyridine as nitrogen sources using the laser ablation method. It was found that the surface contains the pyria group and has a long fluorescent life. Xin et al. [76], based on N-methylpinol, ammonium persulfate, and hydrogen peroxide as raw materials, replaced the strong acid peeling of graphite-synthesis N-GQDs, reducing the residual front-drive body. Qu et al. [77] use citric acid as the carbon source and sulfur as the element to prepare the nitrogen-doped graphene quantum dot (N-GQDs). It has a very high quantum yield and shows excellent optical luminous performance, which can be applied in the field of optical catalysis. Tran et al. [64] use the microwave assistance water thermal method with passion fruit juice and boric acid as raw materials doped graphene to prepare boron-nicotyle-doped graphene quantum dots (B, N-GQDs). It was found that GQDs increase the length and marginal state of effective coexistence and improve the ability to detect tetracycline. With the gradual deepening of the study of nitrogen doping, more and more precursors are used to synthesize graphene quantum dots doped with nitrogen; the most common are citric acid and urea. For example, Yan et al. [78] use citric acid and glycine as raw materials. They are heated to 200 °C with instruments. The obtained liquid is added to a sodium hydroxide solution and continuously stirred, and the N-GQDs are finally synthesized. Martinez et al. [79] use citric acid and glycine as raw materials, syrup solution and sodium hydroxide solution as reagents, mix at a certain temperature, and successfully prepare N-GQDs. It is characterized by the prepared nitrogen-doped graphene quantum dots, and a richer oxygen-containing group was found, which improves the functionalization of use and has a significant improvement in fluorescent performance and launch wavelength. In addition, doped quantum dots and other semiconductor formation composite materials can also further improve the performance of GQDs. For example, Yang et al. [80] used the physical stirring method to synthesize the PD@n-GQDs composite material. Among them, the PDNPS has good decentralization and fine particle size. Compared with PD@GQDs, the current intensity is increased, showing a higher current response and superior electrochemical catalytic activity.

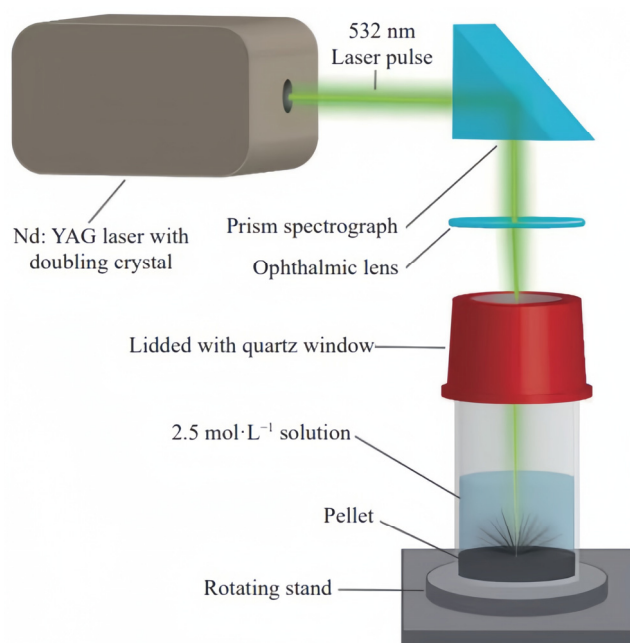


**Figure 12.** Schematic representation of a typical laser ablation set up [75].

### 5.1.2. Phosphorus Doping

Doping phosphorus can change the band structure, electronic structure, and element content of graphene quantum dots and has been shown to be a good way to change their fluorescence properties. Common phosphorus sources include lecithin, phosphoric acid, THPC, ATP [80], Sodium phytate [81], etc. Li et al. [81] used a high-purity graphite rod as the working electrode, platinum and other electrodes, and sodium-plating electrolytes to synthesize P-GQDs as phosphorus sources. In the experiments, the phosphorus mainly existed with the  $C_3PO$  bond, and the  $C_3PO$  key could make the GQDs. The fluorescent performance has been significantly improved. Wang et al. treated lecithin through solvents to obtain phosphorus-doped graphene quantum dots (P-GQDs), which increased quantum yield [70]. Wang et al. [82] used citric acid as the carbon source and sodium-free sodium sulfate water to thermally synthesize P-GQDs. Due to the poor electrical negativeness of phosphorus and sulfur, the transmission rate of electrons is accelerated. GQDs have better performance than unit-element-doped GQDs. Figure 13 shows the synthetic processes and structural illustrations for GQDs and P-GQDs.

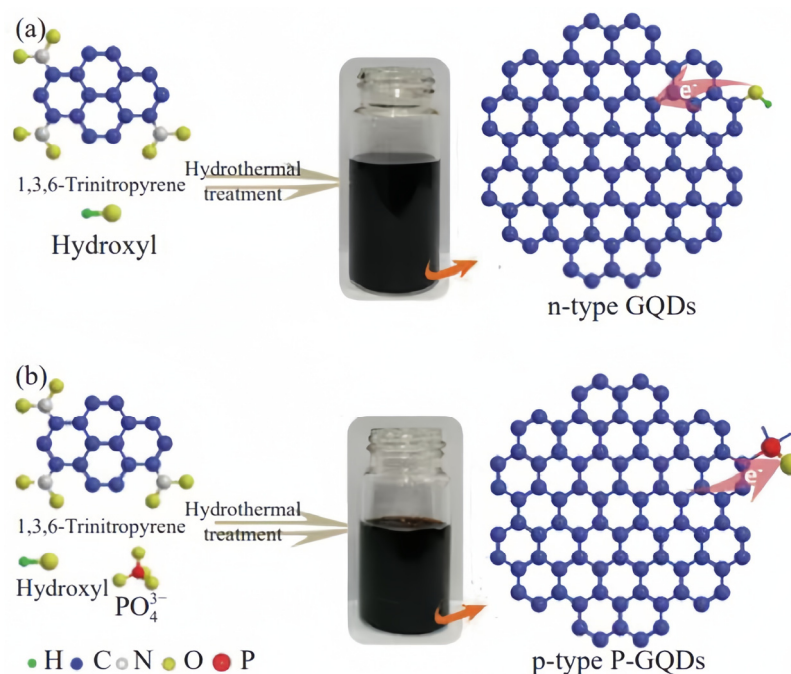


**Figure 13.** Synthetic processes and structural illustrations for (a) GQDs and (b) P-GQDs [83].

### 5.1.3. Sulfur Doping

The sulfur doped into graphene quantum dots mainly exists in the form of C–S–C bonds to improve fluorescence performance and C–SO<sub>2</sub>–C bonds to improve photocatalytic performance. Sulfur can change the band structure of GQDs to increase the path of electron transition, which has great potential in optics. It has been demonstrated in the literature that doping S atoms can provide more energy for photoexcited electrons, which can better regulate the electronic structure and optical properties of nanoparticles [65]. The most common sulfur sources are: 3-cymbal propyate (MPA), Na<sub>2</sub>S [84], cysteine, sulfurate, sulfate [85] and ammonium sulfate. In the work of Luo et al. [86], sulfur powder was used as raw materials to synthesize sulfur doped graphene quantum dots (S-GQDs). He found that there are two ways for sulfur atoms to dope, one is that sulfur atoms replace carbon atoms, and the other sulfur atoms attach to graphene to form a bond state, which will greatly increase the quantum yield. Hasan et al. [87] use cheap and easy glucosamine and thiourea are made of N, S-GQDs through a microwave assisted water thermal method. Fan et al. [84] used NH<sub>4</sub>OH and NA<sub>2</sub>S as the front-drive body to synthesize N,S-GQDs, who found that doping sulfur changed the state of nitrogen, creating more active sites and



## 5.2. Surface Function

Surface functionalization, in a superficial sense, is to make some changes to the surface of graphene quantum dots. It is well known that there are many oxygen-containing groups and hydrophobic  $\pi$ -structural domains on the surface of GQDs that can be used as active sites for surface modification, which can be used to control the surface properties of GQDs, eliminate the non-irradiation complex centers, modulate the fluorescence color of quantum dots, and increase the quantum yield, so that if the oxygen-containing groups are changed reasonably, it will increase the original properties. Therefore, if the oxygen-containing groups are changed reasonably, their original properties will be increased. Surface functionalization is generally divided into two ways: one is to introduce small organic molecules or polymers with strong electron-absorbing efficiency in the process of synthesizing GQDs to change their surface state; the other is to chemically transfer certain groups on the surface of GQDs [11].

### 5.2.1. Hydroxyl Modification

GQDs contain a large number of hydroxyl groups on their surfaces and edges, which can be esterified with carboxyl group-containing polymers, condensed with silane coupling agents, and Kitter reacted with cyano groups to increase the  $\pi$ - $\pi$  conjugated  $sp^2$  structure, which provides the bonding ability for GQDs and increases their conjugated system, thus improving the optical properties. Islam et al. [93] found that by esterization reactions to generate surface defects in GQDs and carbon fiber (CF), the degree of coexistence has been increased to significantly improve the capacitance of composite materials, and the material has broad application prospects in the field of flexible electronic devices. Kang et al. [94] realized the pyridine function of GQDs through the couplet of 3-amino-trice trimethyl oxyxane, and the obtained materials are better dissolved. The reaction of the silane coupling agent with the hydroxyl group of the GQDs yielded amino-functionalized GQDs, and the amidation of the amino group with the carboxyl group of 2,6-bis(pyrazol-1-yl) isonicotinic acid (TpyCOOH) led to the fluorescent GQDs-tpy, which detects metal ions by using the liganding of  $Zn^{2+}$  with the trilobalts, leading to the quenching of the fluorescence by metal-ligand charge transfer. Pourhashem et al. [95] used a silane coupling agent as a bridge between GQDs and epoxy resin. XPS showed that C-Si and Si-O-Si bonds appeared at 283.6 eV and 532.7 eV, respectively, indicating that the silane coupling agent was involved in the above reaction. Due to the interfacial interaction between the two surfaces to improve the specific surface area and structural compatibility, the maximum emission wavelengths at 460 nm were observed under the excitation of 420 nm, which increases the optical properties of the product. Zhang et al. [96] used Kitter's reaction to functionalization of GQDs, which can change its electrical performance by changing the degree of cross-linking between the two. The preparation process is shown in Figure 15. Through the surface active sites provided by GQDs, the low-cost and highly tunable composites are utilized to expand the  $sp^2$  structure of the  $\pi$ -conjugation and enhance the conjugated system after crosslinking with carboxyl groups, silane coupling agents, and cyano groups through esterification, condensation, and Kitter reactions, which clearly exhibit good maximum emission wavelength and other properties.

### 5.2.2. Carboxyl Base Modification

The surface of GQDs also contains a large number of carboxyl groups, which can undergo esterification and amidation reactions with hydroxyl groups, amino groups, etc., and produce more active sites through conjugation to increase their electrical properties. Chan et al. [97] used GQDs carboxyl group and amine functional  $TiO_2$  reaction to covalent prices to prepare GQDs/ $TiO_2$  composite materials. Under visible light irradiation, GQDs generate electrons and transfer them directionally to the  $TiO_2$  surface, facilitating photo-generated charge separation, which effectively improved its optical performance. Cho [25] et al. reduced the strong conjugated interaction between GQDs by grafting hexylamine and significantly inhibited the aggregation of GQDs. The diagram of the modification is shown

in Figure 16. The amphiphilic nature of the modified GQDs, most of which are located at the interface between the water and organic phases, allows the Pickering emulsion to remain stable for several months; it was also found that the fluorescence emission of the GQDs is caused by the radiative decay of excited electrons from the lowest unoccupied molecular orbital (LUMO) at the jagged edges of the GQDs to the highest occupied molecular orbital (HOMO). Tachi et al. [98] used phenolic hydroxyl groups and GQDs carboxyl genetic reactions, effectively suppressing non-radiation reorganization, significantly accelerating the transfer of photocopy electronics, and increasing its quantum production rate. By grafting different materials to undergo amidation and esterification reactions and adding catalysts such as EDC to accelerate the reaction rate, the chemical structure of GQDs was significantly altered, and the integrity of the surface  $\pi$ -electron network, optical properties, and surface stability were enhanced.

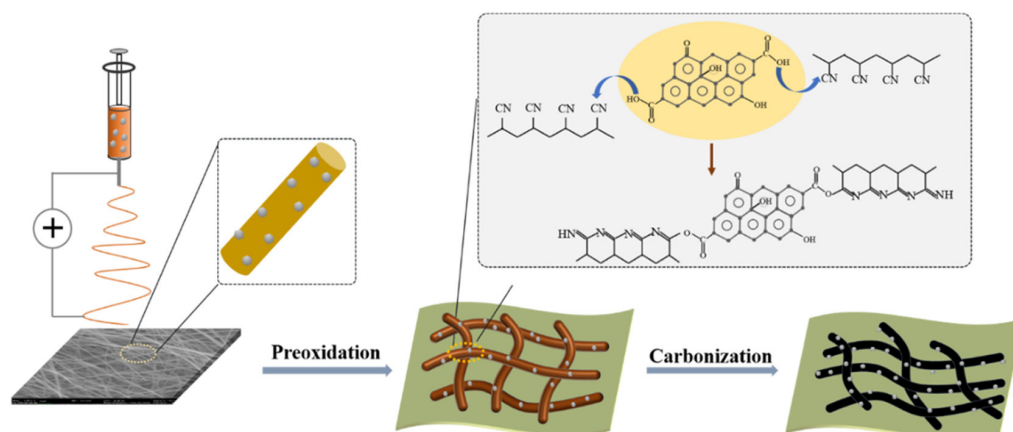


**Figure 15.** Schematic illustration of the preparation procedure of GCNF mats [96].

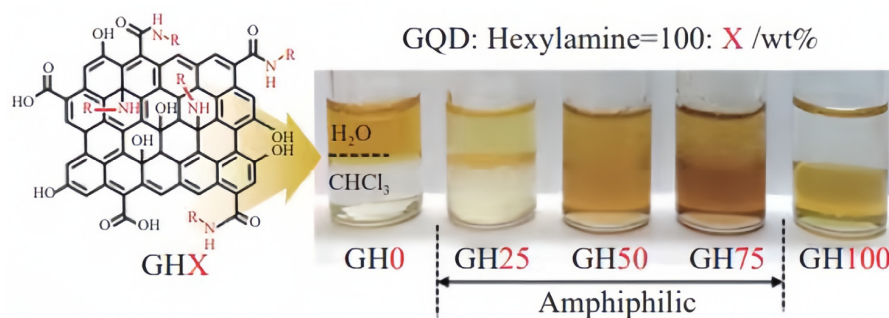


**Figure 16.** Surface-modified GQDs with hexylamine [25].

### 5.2.3. Aromatic Ring Modification

Direct grafting of molecular chain segments on the aromatic ring structure of GQDs themselves by the Gomberg–Bachmann reaction, the olefin epoxidation reaction, and the Huisgen reaction was used to improve the fluorescence properties of these GQDs. The resonance effect between the grafted molecular chain segments and the GQDs produces defective states in the band gap, which effectively modulates the photoluminescence of the quantum dots, improves the quantum yield, and systematically tunes the fluorescence properties of the GQDs. Guan et al. [99] used the Gomberg–Bachmann reaction between the NN triple bonds on the aromatic rings containing different substituents, such as aniline, sulfonine, 4-aminobenzoic acid, and 5-amino-1-naphthalene sulfonic acid, which exhibited bright blue, yellow-green, green, cyan, and other fluorescences, respectively, and found that especially the aromatic rings containing sulfonic acid groups could greatly increase the QY of GQDs. The coupling of individual electrons in the  $\delta$  orbital of aryl groups converted from diazo ions and aromatic ring double bonds of GQDs produces defect states,

which improves the efficiency of electron-hole recombination. Carbon-carbon double bonds are prone to providing electrons and being oxidized, so Wang et al. [100] used hydrogen peroxide as an oxidizing agent to break the aryl ring double bonds through an electrophilic addition reaction, forming epoxy functional groups on the surface of the GQDs, which enhances the surface activity and broadens the range of light absorption at 400~450 nm, expanding their applications in bio-imaging and photothermal therapy. The discovery by Hossain et al. [101] that graphene can be modified in situ by the diazotization reaction of amines opens up new chemical avenues for the functionalization of graphene. Various other reactive functional groups introduced through this reaction can be used to trap and immobilize metal atoms or bioactive molecules. The specific process is shown in Figure 17. Graphene quantum dots broaden light response by increasing structural conjugation via the Gomberg-Bachmann reaction, olefin epoxidation, and the Huisgen reaction.

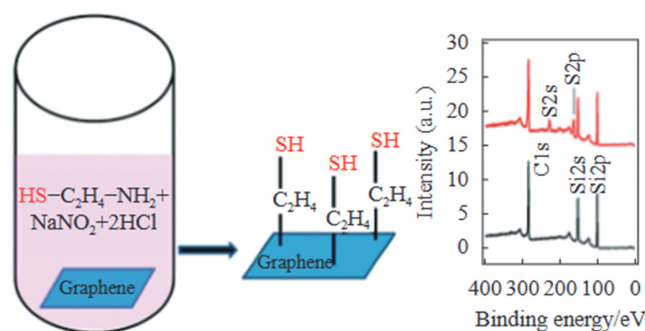


**Figure 17.** Amine-derived diazonium salts undergo spontaneous in situ reduction on graphene preloaded [101].

#### 5.2.4. Other Modifications

In addition to the typical graft modification using carboxyl and hydroxyl functional groups on the surface of GQDs as described above, researchers have also investigated other modification methods. Ge et al. [102] first prepared GQDs electrochemically, then added  $\text{H}_2\text{O}_2$  and stirred under UV light irradiation for 24 h to obtain hydroxylated graphene quantum dots (H-GQDs), which showed stronger C-OH peaks in the infrared spectrum; after the oxidation, some broken  $\pi$ -conjugated electronic structures in the GQDs were reorganized, which led to an increase in  $\pi$ -electron leaving domains, making it easier to be The fluorescence intensity of H-GQDs is 5.5 times higher than that of GQDs due to the deprotonation of the functional groups on the surface of GQDs, which are negatively charged, and monodispersion is achieved by the repulsion of the negative charge. Ashraf et al. [103] prepared  $\text{Cu}_2\text{O-CuO@GQDs}$  with a core-shell structure in the presence of sodium dodecyl sulfate by taking advantage of the electrostatic interactions existing between the negatively charged GQDs and the positively charged hexagonal  $\text{Cu}_2\text{O-CuO}$ . The material exhibits excellent electrocatalytic properties with a high specific surface area and high electrical conductivity.

#### 5.3. Composite Material

Composite materials are solid materials made of two or more pure or homogeneous substances that have superior performance to the original single This material is superior to the original single material and has a comprehensive effect. Organic materials have particular advantages, such as easy film formation, high carrier mobility, etc., which can greatly complement the performance of GQDs and will lead to many new applications. In recent years, there has been increasing interest in developing new GQD composites [104]. Distributing other semiconductor materials on the surface of GQDs or between the layers to form a composite material with graphene as the matrix, using its excellent electrical conductivity, fast electron transport, and other properties to improve performance, accelerate the separation rate of electron-hole pairs, inhibit the non-radiative recombination of the two, enhance their optoelectronic properties, and expand the scope of their applications, is

an effective way to improve the performance of the composite material. Many materials have been applied to form composites with GQDs, and these composites have shown the ability to improve and optimize device performance. According to their composition, GQDs are broadly categorized into the following three types: undoped GQDs composites, single-doped GQDs composites, and double-doped GQDs composites.

### 5.3.1. Undoped GQDs Composites

Undoped GQDs composites are composites formed directly from GQDs and other semiconductors, and under the condition of light excitation, the valence band electrons of the semiconductor receive energy to jump to the conduction band, leaving holes in the valence band, and the electrons are transferred to the conduction band of the other semiconductor, thus realizing a large number of electron transfers, narrowing the photo-generated bandgap, and expanding the photoresponse to the visible range. He et al. [105] first used polyacrylonitrile nanofibers (PAN) as a substrate in situ to prepare BiOI/PAN composite fibers, with BiOI sheets arranged vertically and uniformly around the PAN to form a hierarchical structure on its surface. Then, GQDs were sprayed onto the BiOI surface to form S-type heterojunctions. The degradation performance of the composite for phenol was significantly improved by the combined effect of the fiber hierarchical structure and S-type heterojunction. Zhang et al. [106] prepared composites of GQDs and reduced graphene oxide (rGO) with a unique three-dimensional structure and found that the GQDs/rGO complexes were more active than GQDs and rGO in the reduction of nitroaromatics, and their catalytic performance was closely related to the ratio of GQDs to rGO in the composites, with the defects and the edges being the active sites, and the mass ratio of GQDs to rGO was 1:4. The mass ratio of GQDs to rGO of 1:4 showed the highest catalytic activity. In addition, the catalytic performance is also attributed to the unique 3D network structure, which facilitates the adsorption of reactants and the diffusion of products. Goswami et al. [107] synthesized GQDs/ZnO/GaN-NT composites by uniformly dropping GQDs into ZnO/GaN-NT and spin-coating (4000 r/min) at 200 °C. It was found that the effective introduction of GQDs could act as an incident ultraviolet absorber and electron hole generator, and the energy band structure could be tuned for better charge transport. The specific process is shown in Figure 18. Through the direct composite of GQDs with other semiconductor materials, GQDs composites combine the advantages of graphene, quantum dots, and oxide semiconductors, which is not only a simple process but also effectively accelerates electron transfer by increasing photogenerated carriers, improves the separation efficiency of electron-hole pairs, and better absorbs the energy so as to improve the photocatalytic activity. GQDs composites provide a good design route for photocatalysts, and there is room for long-term development.

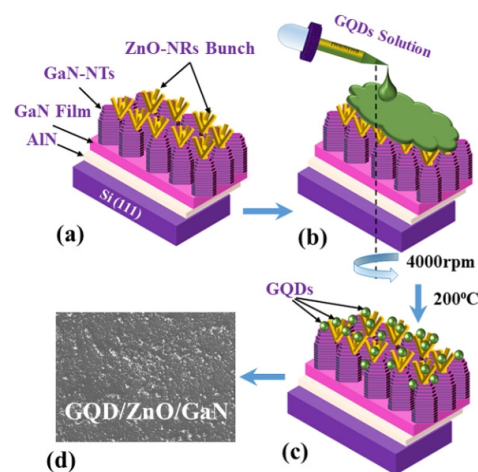


**Figure 18.** Schematic diagram of the (a–c) fabrication process of the GQD-sensitized ZnO-NR/GaN-NT heterostructure, (d) SEM image of the GQD/ZnO-NR/GaN-NT heterostructure [107].

### 5.3.2. Single-Doped QDs Composites

Doping can effectively change the electron density of semiconductor materials, reduce the exciton binding energy and the lowest unoccupied molecular orbitals of QDs, and further composite with semiconductor nanoparticles to efficiently inhibit the non-radiative recombination of electron-hole pairs and relatively improve the catalytic performance. Therefore, theoretically, the doped QDs and other semiconductor composites coupled with close contact can improve the photocatalytic activity of electron-hole pair separation and redox reactions. Yang et al. [108] first synthesized heterojunctions by ultrasonically mixing QDs with  $\text{BiVO}_4$  before using the hydrothermal method. Due to the energy level effect of nitrogen atoms, they can increase the mobility of photogenerated electrons, thus improving their photocatalytic activity. On this basis, Li et al. [109] synthesized N-QDs/ $\text{TiO}_2$  composites using a hydrothermal method, and the N-QDs showed stronger absorption peaks in the UV range than the QDs, which significantly improved the photocatalytic performance. The contents of pyridine N and graphite N were as high as 22.47% and 31.44%, respectively, when the content of ammonia was added at 50 mL, and the photocatalytic activity was about 95% after 12 min. This indicates that pyridine N and graphite N play an important role in photocatalytic performance. The composite of nitrogen-, sulfur-, and phosphorus-doped graphene quantum dots with other semiconductor materials has certain advantages over other single materials, and the resulting multi-energy level effect promotes interfacial charge transfer, prolongs the charge lifetime, and reduces the photoresist effect. Meanwhile, the electron-hole-pair composite rate in the QDs composite material decreases, and its emission spectra and luminescence efficiency can be greatly changed, and it can be used as a kind of high-efficiency photocatalyst.

### 5.3.3. Double-Doped QDs Composites

The double-doped QDs introduce different energy levels of nitrogen, phosphorus, and sulfur states during the photocatalytic reaction, which can better absorb visible light to generate electron holes based on the difference in their ability to transport electrons, and the heterojunctions formed by the composites significantly inhibit the light-induced carrier recombination due to the charge-differential coupling effect of the diatom, which exhibits excellent catalytic activity. Li et al. [110] prepared nitrogen-sulfur co-doped graphene quantum dot (NPG)/ $\text{Bi}_5\text{O}_7\text{I}$  nanocomposites by solvent-thermal method, which can more effectively improve the ability of QDs to utilize light under light irradiation, and the electrons of  $\text{Bi}_5\text{O}_7\text{I}$  will also be transferred to the surface of NPG, which will enhance its reducing properties. The transfer of a large number of electron hole pairs in the composite was utilized to effectively improve the photocatalytic degradation ability. Cai et al. [111] fabricated N,S-QDs/ $g\text{-C}_3\text{N}_4$  composites by physical stirring, which enhanced the visible light absorption ability of the composites, and the photogenerated electrons could be effectively transferred to the N,S-QDs due to the interfacial contact formed between the  $g\text{-C}_3\text{N}_4$  and the N,S-QDs, which indicated that the visible-light-driven photocatalytic activity has been effectively improved, and it can also be said that there is a tendency for quenching of the fluorescence intensity after the addition of the quantum dots. Tian et al. [112] used the same method to form composites of N,S, and QDs with reduced graphene oxide/titanium dioxide nanotubes (RGO/ $\text{TiO}_2\text{NT}$ ). The UV-Vis absorption spectra showed C=N, C=S, and S=O peaks at different wavelengths, which broadened the range of light absorption. The pollutants were adsorbed on the surface of the catalysts to be oxidized indirectly by hydroxyl and superoxide radicals, and the narrowing of the bandgap was attributed to the formation of the Ti-O-C chemical bond between  $\text{TiO}_2\text{NT}$  and RGO. The doubly doped QDs enhance the absorption of visible light through the introduction of multi-energy-level energy states, improve electron conduction and diffusion, and act as sensitizers to improve the spectral absorption of the composites. It does not affect the synthesis of a single semiconductor, and due to the presence of energy level differences, the composites formed, which effectively enhance the binding force and significantly inhibit carrier recombination, exhibit smaller band gaps than the singly doped QDs and obtain

good visible light absorption, thus significantly accelerating the degradation of pollutants. In conclusion, GQD composites can be good for improving and optimizing the performance of devices. New GQD functions can be developed by utilizing doping, composites, and other techniques, which will open up new application areas for GQDs [104].

## 6. Application Field of Graphene Quantum Dots

GQDs have important application potential in many fields, and his current research focuses on several areas, such as catalysts, biomedicine, sensors, and photovoltaics. This article will briefly introduce its catalysts and photovoltaic devices and focus on various sensors and biomedical aspects, such as bioimaging, tumor treatment, etc.

### 6.1. Catalyst

GQDs have some specific chemical groups that make them catalytic, and the electron-hole pairs generated by semiconductors under illumination have redox ability. GQD can improve the performance of catalysts by promoting charge transfer, accelerating the separation rate of electron-hole pairs, or enhancing photoadsorption [113]. Li et al. [39] prepared products to launch Blue-ray and have electrocatalytic activity. In an alkaline medium catalytic oxygen reduction reaction (ORR), its catalytic activity is equivalent to that of commercial PT/C catalysts. Liu et al. [114] mixed N-GQDs and  $\text{Bi}_2\text{Ti}_2\text{O}_7$  for 60 min to form composite materials. Electron transfer from  $\text{Bi}_2\text{Ti}_2\text{O}_7$  to N-GQDs and holes to  $\text{Bi}_2\text{Ti}_2\text{O}_7$  effectively promotes the separation of electron-hole pairs, increases the electron transport rate, and improves the degradation performance. Qu et al. [32] prepared nitrogen-doped graphene quantum dots with oxygen-rich functional groups by introducing nitrogen atoms in situ in GQD by electrochemical method using an acetonitrile solution containing tetrabutylammonium perchlorate as an electrolyte, and the prepared GQDs had photocatalytic properties. Yang et al. [108] compounded N-GQDs and  $\text{BiVO}_4$  to form a heterojunction and used the superoxide free radicals generated by the composite material to degrade the methyl blue, and it was found that the main oxidant comes from the OH of the N-GQDs and not the hole of the  $\text{BiVO}_4$  valence band. What is generated shows that the introduction of N-GQDs in this composite material improves the efficiency of optical conversion, inhibits the recombination of electron-hole pairs, and greatly improves the degradation ability. Zhu et al. [31] used  $\text{BiOCl}/\text{BiVO}_4/\text{N-GQDs}$  for tri-heterogeneous heterolytic high-efficiency degradation of BPA. Their schematic diagram and the charge separation process under visible light irradiation are shown in Figure 19. The introduction of nitrogen effectively accelerated the electronic transmission rate and accelerated the electronic acupoint pair through the synergy of three components. The separation shows excellent degradation performance. Figure 20 is the ORR performance test diagram of the composite material catalyst.

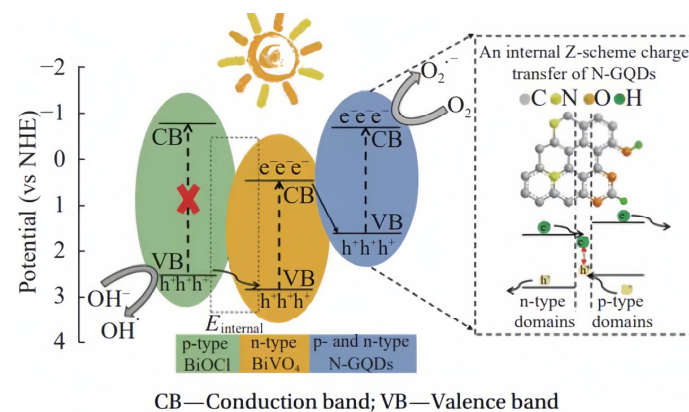


**Figure 19.**  $\text{BiOCl}/\text{BiVO}_4/\text{N-GQDs}$  Tri-Heterogeneous Kinsene and the charge separation process of the charge under visible light (embedded: internal Z schemes of N-GQDs composed of type P and N domain transmission) [115].

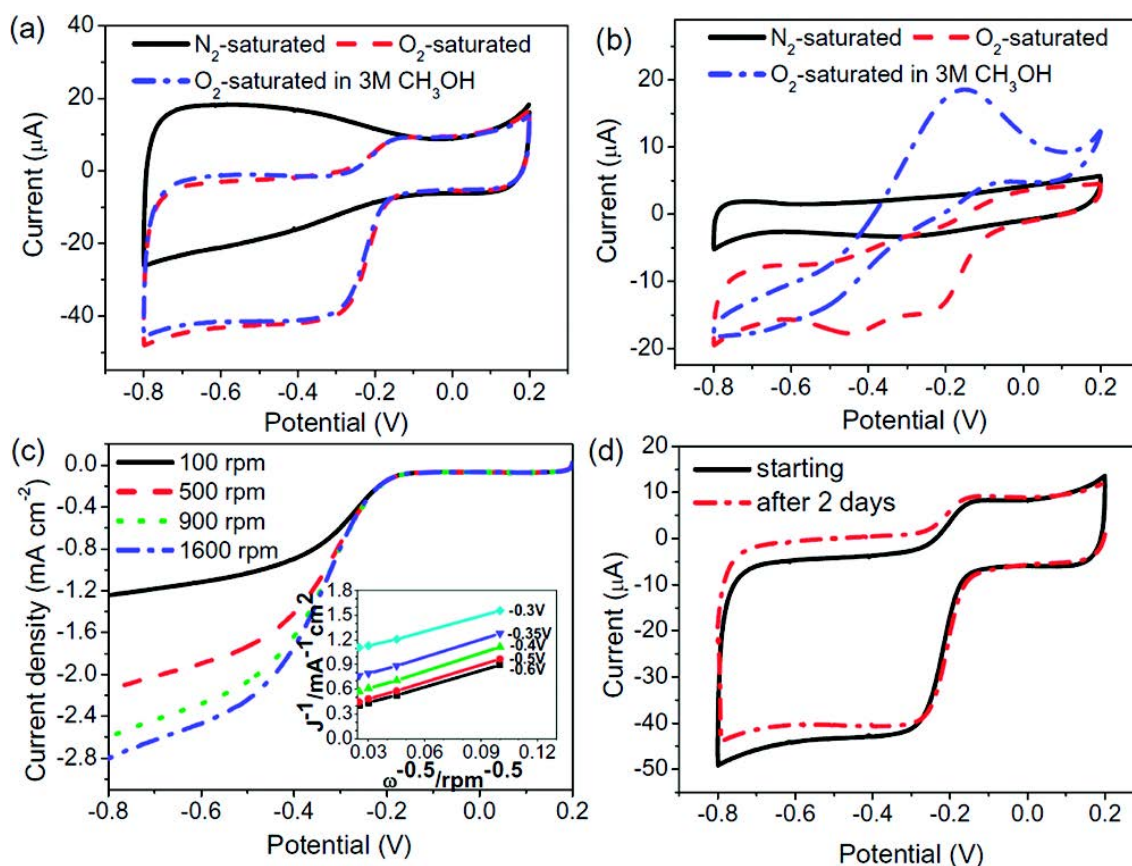


**Figure 20.** (a,b) Cyclic Voltammetry (CV) curves of (a) N-GQD/graphene and (b) commercial Pt/C on a GC electrode in N<sub>2</sub>-saturated 0.1 M KOH, O<sub>2</sub>-saturated 0.1 M KOH, and O<sub>2</sub>-saturated 3 M CH<sub>3</sub>OH solutions. (c) Rotating disk electrode (RDE) curves for N-GQD/graphene in O<sub>2</sub>-saturated 0.1 M KOH with different speeds. The inset shows the Koutecky-Levich plots derived from the RDE measurements. (d) Electrochemical stability of N-GQD/graphene as determined by continuous cyclic voltammetry in O<sub>2</sub>-saturated 0.1 M KOH [116].

## 6.2. Photovoltaic Device

Due to the excellent optical and electrical properties of GQDs and their application cost, they have potential application prospects in the fields of organic light-emitting diodes, high-performance photovoltaic devices, such as organic-inorganic hybrid solar cells, dye-sensitized solar cells, and organic light-emitting diodes. Yan et al. [83] reported that GQDs have good optical absorption ability and optimized absorption in ultraviolet and visible light zones. In addition, the computationally simulated band model of GQDs shows that when GQDs obtain an electron from I<sup>-</sup>, they have the ability to inject electrons into the wide bandgap of TiO<sub>2</sub>. In addition, they have also discovered the application value of GQDs in photochemical cells, especially near-infrared light, which has made their application range in the optical field larger. Li et al. [117] mix green fluorescent GQDs and electronic receptor polymers and make thin-film solar cells. Figure 21a is a device schematic diagram. Figure 21b,c are test devices. Light current-voltage (J-V) curve charts They are divided into two groups, namely the original sample group and the addition of 10 wt% of the GQDs group. After experimentation, the latter's photoelectric performance was significantly improved. Gupta et al. [118], mixing GQDS and P3HT or MEH-PPV co-mixing polymer components, Compared with GS and the commonly used polymer devices, the efficiency of solar batteries and their organic light-emitting diodes have greatly improved at the same time. These studies all prove the application potential of graphene quantum dots in the field of batteries or diodes.

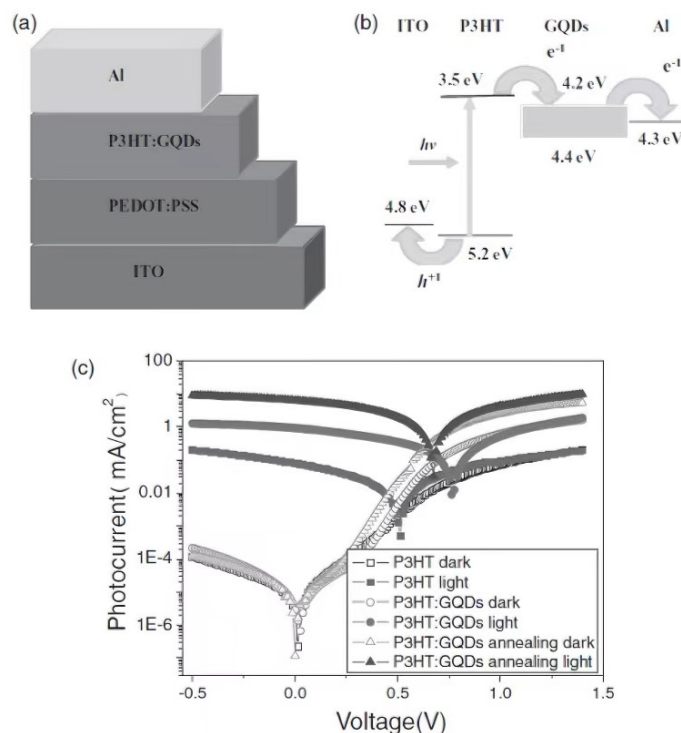


**Figure 21.** (a) Schematic device structure of P3HT active layer polymer solar cell doped with GQDs; (b) Energy band diagram; (c) J-V characteristic curve [117].

### 6.3. Sensor

#### 6.3.1. Graphene Quantum-Point Photoelectric Chemical Sensor

GQDs have active functional groups on the surface, autofluorescence performance, and superior theoretical conductivity, which can be used as a substance connected to biological probes on electrochemical biosensors or directly capture metal ions. They have also been used in electrochemistry. SSDNA molecules can interact with graphene quantum dots, and together they can be used as probes to prepare electrochemical sensors. Zhao et al. [119] based on the strong interaction between ssDNA and graphene materials, using the pyrolytic graphite electrode modified by graphene quantum dots and the ssDNA molecule of a specific sequence as a probe, the principle of action is that when the reaction between ssDNA and GQDs occurs, a strong bonding force will be generated, which will inhibit the electron transfer between the electrochemically active substance  $[\text{Fe}(\text{CN})_6]^{3-/4-}$  and the electrode, which will weaken the signal. When paired DNA appears, it can bind to ssDNA, which in turn increases the electrical signal. Ran et al. [120] combined nitrogen-doped quantum dots with cobalt oxide to form a complex, which was then combined with the antibody modified by the golden nanoparticles to build an electrified student material sensor that can be used to detect human epididymal proteins. The linear range is 0.002~20 ng/mL, and the detection limit is 1.5 pg/mL. Zhang et al. [121] prepared an electrochemical luminous biosensor based on the T7 nucleic acid external enzyme auxiliary cycle amplification and DNA-mediated silver nanoparticles for analysis of Microsna. The schematic diagram of the electrochemical sensor they use is shown in Figure 22. Wang et al. [122] developed a photoelectric student material sensor through the energy transfer between carbon quantum dots and gold nanoparticles. Two miRNAs were detected by two hairpin probes modified on Aunp. Ions can be detected with electrochemical sensors. For example, Chen et al. [123] used graphene quantum dots and  $\text{S}_2\text{O}_2^{8-}$  to build a sensor to detect  $\text{Cr}^{6+}$  in water samples. There are also studies using doped graphene quantum dots as electrochemical sensors. Qu et al. [124] developed, through N-doped GQD, a high-sensitivity fluorescent biosensor for tyrosinase (TYR) and acid phosphatase (ACP)

activity. Cui et al. [125] prepared new N- and S-doped GQDs and developed composite-based complexes.

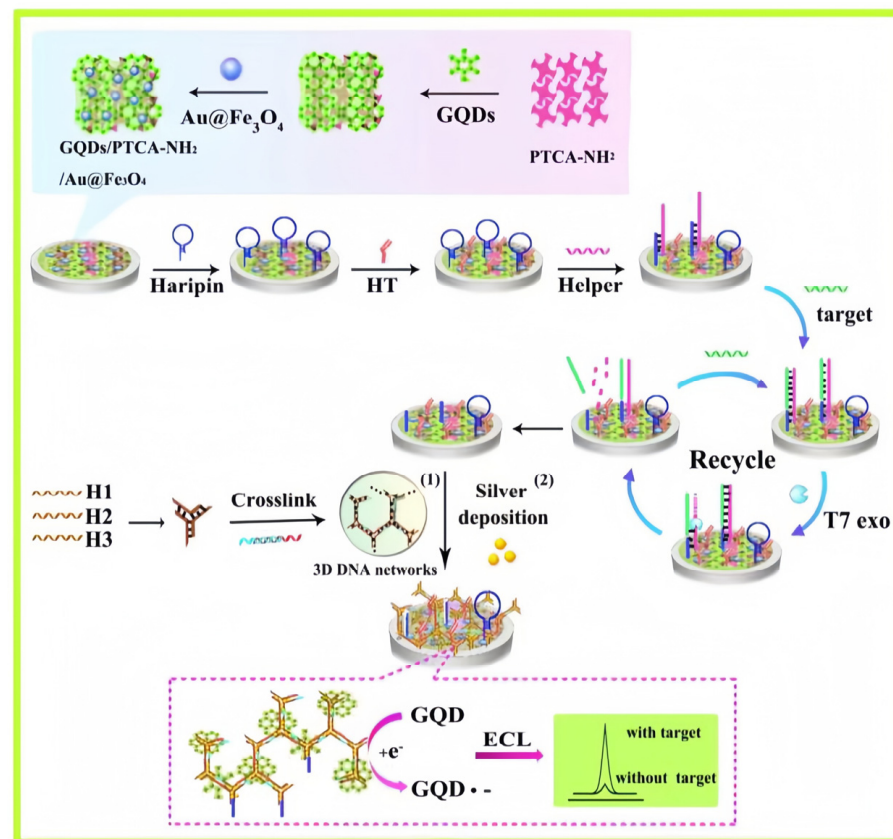


**Figure 22.** Schematic of a graphene quantum dots-based electrochemical sensor [121].

### 6.3.2. Gas Sensor

Gas sensors are mainly divided into semiconductor gas sensors and optical gas sensors. The styles generally include flat-screen [16], tube [126], and film type [127]. Their shape is shown in Figure 23. The working principle of the two sensors is also different. Gas sensors mainly determine the gas concentration by testing the gas to give and receive electrons on the surface of sensitive materials to determine the resistance or current change. The working principle of the optical sensor is to determine the absorption of the wavelength by determining the sensitive material in the gas [128]. In order to enhance the gas-sensitive properties of traditional materials, graphene quantum dots are generally combined with traditional sensitive materials in the form of doping or blending. On the one hand, GQDs are P-type semiconductors, and when combined with N-type semiconductors, PN junctions are generated, which can adjust the resistance of the sensor [129]. Secondly, GQDs have the characteristics of high mobility, and their doped heteroatoms and functional groups also play a role in electron migration. These properties enhance gas sensitivity, which we illustrate with NH<sub>3</sub> gas sensors and NO<sub>2</sub> gas sensors.

As a polar molecule, NH<sub>3</sub> easily interacts with GQDs reactions, causing a sensor response. Arunragasa et al. [130] took pyrene as the raw material, using the hydroxyl-based GQDS to study the sensitive characteristics of OH-GQDS to 8 different gases, and found that the sensor has excellent sensitivity and selectivity to NH<sub>3</sub>. The N atom in NH<sub>3</sub> has the strongest response to the hydroxyl group. Chen et al. [16] used the prepared GQDs to study the sensitivity of NH<sub>3</sub> at room temperature and experimentally prepared the sensor with two different sets of samples, namely GQDs solutions with pH 5 and pH 7, and the results were completely different. Firstly, the response value of the sensor with a low pH value is greater than that of the other group, and the resistance of the sensor prepared with acid in

$\text{NH}_3$  decreases, and the resistance of the sensor prepared with neutral preparation increases, and the effect is greater in the presence of water. This is because sensors prepared with acidic solutions will have a large number of carboxyl groups on their surface to increase the resistance, and in the case of relative humidity, it will react with  $\text{NH}_3$ , and a large number of carboxyl groups will be deprotonated, which will lead to a decrease in resistance, so the regulation of  $\text{NH}_3$  can be realized. Polymer sensors have always been limited in their range of applications due to some disadvantages, but when combined with GQDs, their gas-sensing performance can be greatly enhanced. Gavvani et al. [131] used the prepared sulfur and nitrogen-doped graphene quantum dots to compose with polyiline and deposit on a flexible polytic dilately glycolic film as a sensor. Studies have found that under the same  $\text{NH}_3$  concentration, the performance of the doped sensor is much greater than before doping. This is because the doping of the atom will enhance the concentration of the cave load and enhance the interaction between molecules. The performance of different gas sensors is shown in Figure 24, and the parameters of  $\text{NH}_3$  gas sensors based on GQDs are listed in Table 3.

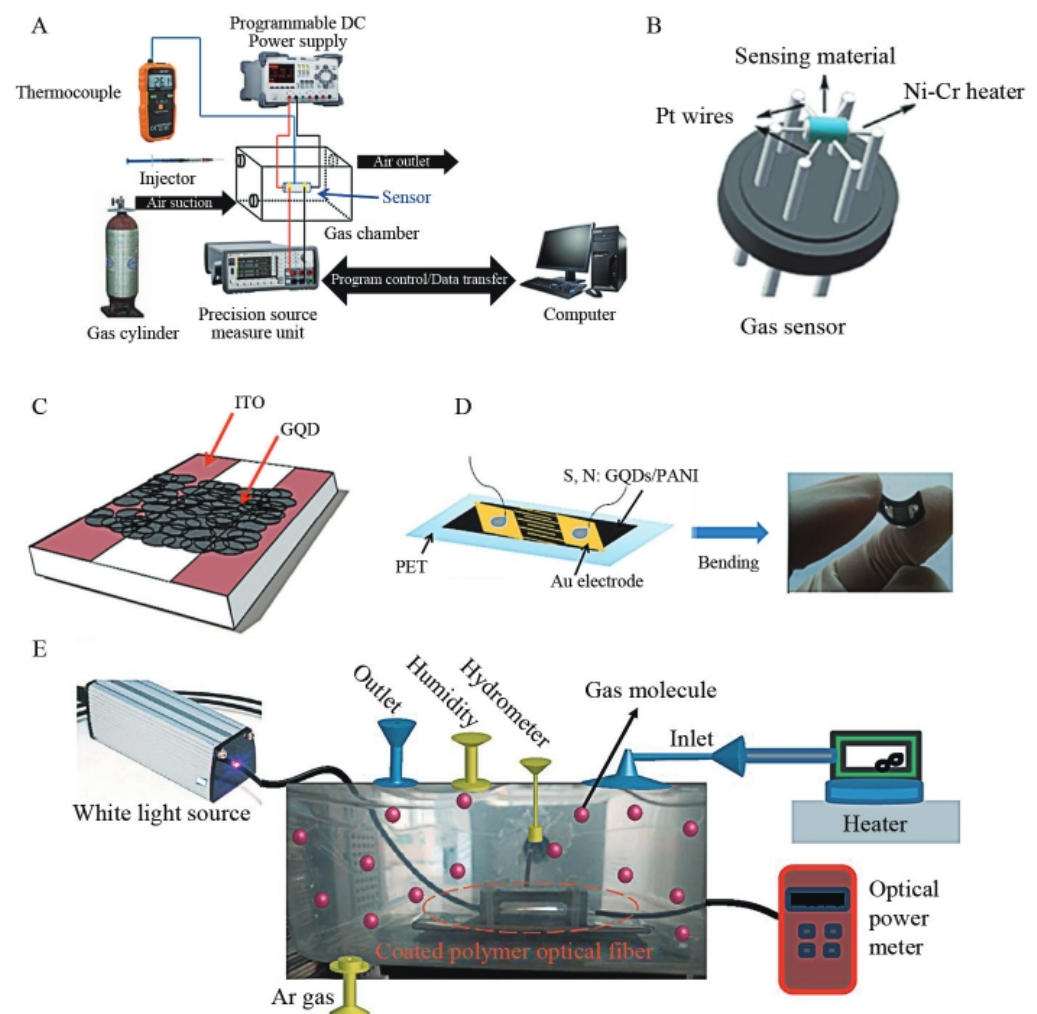


**Figure 23.** (A) Schematic diagram of semiconductor gas sensor test system [127]; (B) Schematic diagram of gas sensor device: Tubular [126], (C) Planar [16], and (D) Thin film type [127]; (E) Schematic diagram of optical gas sensor test system [128].

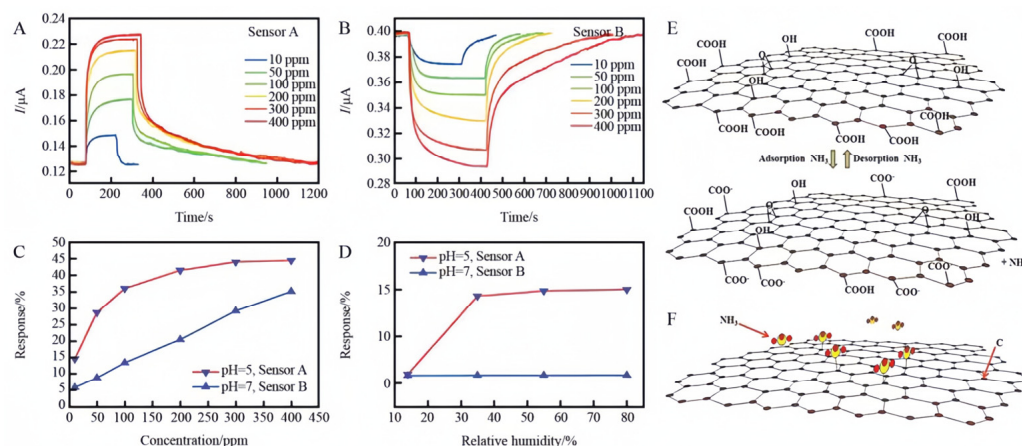


**Figure 24.** Current responses of (A) sensor A and (B) sensor B with different concentrations of  $\text{NH}_3$  [16]; (C) Response concentration curves of sensor A and sensor B [16]; (D) Response changes of sensor A and sensor B to 10 ppm  $\text{NH}_3$  in different humidity [16]; and (E) acid sensor A [16] and (F) neutral sensor B [16].

**Table 3.** Summary of performance parameters of  $\text{NH}_3$  gas sensors based on GQDs.

Sensing Materials	Temperature	Gas Concentration (ppm)	Sensitivity (%)	Response/Recovery Time	Ref.
GQDs	Room temperature	10~400	14.9~44.5	26/21 s	[16]
OH-GQDs	Room temperature	10~500	1.54~76.63	64/69 s	[130]
S,N:GQDs/PANI	Room temperature	100~1000	42~385	115/44 s	[131]
N-GQDs/PEDOT-PSS	Room temperature	1500	212.32	6.8/9 min	[132]
N-GQDs/PANI	Room temperature	1500	110.92	7.0/0.083 min	[87]

There are many studies on  $\text{NO}_2$  gas sensors. Abbasabadi et al. [133] prepared a Fe-doped reduction oxygenic graphene quantum dot material for  $\text{NO}_2$  gas detection. The research results indicate that the mixed materials have a larger volume and surface area. Doping with other atoms will also produce more electron-hole pairs on the surface of graphene quantum dots, improving the electronic properties of the material. Lv et al. [134] prepared N-GQDs-modified three-dimensional pores  $\text{In}_2\text{O}_3$  and  $\text{SnO}_2$  to test the response value of the sensor to  $\text{NO}_2$ . N-GQDs and these materials will form heterogeneous knots, and the unique structure and holes of these materials also increase the spread of the diffusion, so the doped graphene quantum point will have a better response value for  $\text{NO}_2$ .

### 6.3.3. Optical Sensor

Since graphene quantum dots can induce signal changes by binding to metal ions, GQDs optical sensors have been widely used for detection [135–137]. The doped GQDs have stronger fluorescence properties and also make the detection range wider. Das et al. [138] used oxide graphene as the carbon source, taking Dimethylformamide as a solvent. The solvent-thermal method is used to synthesize nitrogen-doped graphene quantum dots. Due to the presence of hydroxyl groups inside the functional groups of GQDs, they can assist gold particles in detecting trivalent iron ions. Optical sensors can also be used as bioprobes. The role of GQDs in biosensing is to detect and indicate the presence of biomolecules, which works on the principle that the combination of the detected biomolecule with a specific functional group on top of the graphene quantum dots changes the fluorescence properties of the GQDs, which can be utilized to detect certain biomolecules. Shi et al. [139] developed a biosensor using GQDs in conjunction with AuNPs for the detection of *S. aureus*-specific gene sequences. The carboxyl groups on

the surface of the QDs were first activated using conventional carbodiimide chemistry, and the QDs were modified with aminated ssDNA. These aunp were also modified with a thio-DNA probe, which, if sequences from the target staphylococcus were present, would bridge the gap between the probe sequences on the QDs and the probe sequences on the aunp to bring the two close enough together to allow energy transfer to occur. With the addition of the target oligonucleotide, the fluorescence signal will have a much higher fluorescence bursting efficiency. This illustrates the power of explicit modification of QDs in biosensing.

#### 6.4. Biological Field

The *in vitro* and *in vivo* toxicity of graphene quantum dots (GQD, ultra-small GO of 3–5 nm) was studied, and the effect of graphene oxide (GO) size on its biotoxicity was studied using GO at 20–30 nm as a control. The results of WST, ROS reactive oxygen species, and Annexin apoptosis detection showed that GQD had no obvious cytotoxicity at concentrations as high as 600  $\mu\text{g}/\text{mL}$ . *In vivo* distribution, tissue sections, and blood biochemistry The results of the blood routine and other experiments showed that GQD is rapidly excreted from mice and has no significant effect on growth. GO accumulates in the liver and spleen of mice and causes death in some mice after multiple administrations. These studies show that graphene quantum dots have good biosafety and biocompatibility, and graphene size has a certain impact on their accumulation in organisms and the resulting toxicity [28]. Toxicity studies against GQDs are shown in Figure 25.

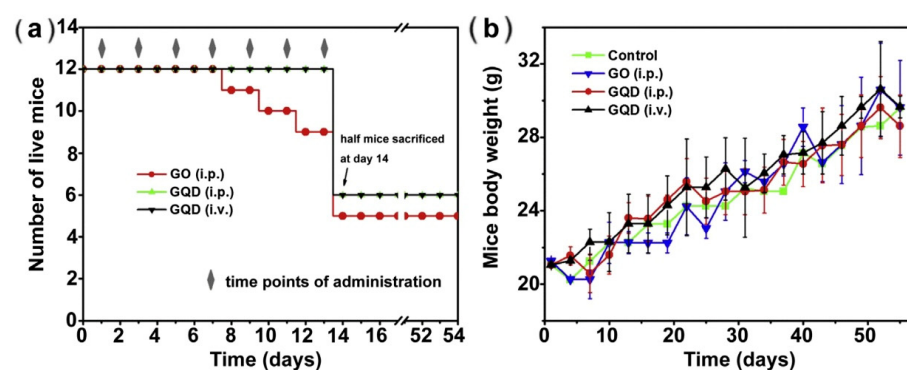


**Figure 25.** (a), Mice were injected seven times with GQD-PEG and GO-PEG, respectively, and three of them died from multiple injections of GO-PEG. Half of the survived mice were sacrificed after 1 day of injections for the study of short-term toxicity; (b), the survived mice were weighted every three days, and no difference from the control group was observed [28].

##### 6.4.1. Cancer Tumor Treatment

The use of GQDs in cancer therapy can be categorized into three categories: photodynamic therapy, photothermal therapy, and drug delivery systems.

Optical therapy is a minimally invasive treatment. Due to its high degree of selectivity for tumors, it is widely used in the clinical treatment of various cancers [140,141]. Effective PDT requires 3 key components: Photosensitizer, light, and oxygen. The synergistic effect between the three can generate reactive oxygen species, among others, and can initiate related transcription factors through apoptosis. There are many scholars who have used different cells to validate the toxicity of graphene quantum dots, and since photosensitizers are usually harmless in the absence of light, tumor therapies can be specifically targeted by selective illumination, limiting damage to surrounding healthy tissue. Ju et al. [109] synthesized the GQD optical agent of N atomic doping by the thermal decomposition method and controlled the generation of GQD-activated oxygen by controlling N-doped amounts to achieve efficient PDT. It was found that increasing the number of doped nitrogen atoms could significantly increase the yield of reactive oxygen species. In addition, NGQD-DOX-APTES were prepared by conjugate modification of the quantum dot surface

for nuclear-targeted drug delivery via charge inversion, which can be used as drug carriers and photosensitizers to achieve nuclear-targeted drug delivery and simultaneous release of reactive oxygen species in high concentration. This offers a promising strategy for the development of multifunctional nanobiomedical therapeutic platforms. The application of graphene in tumor treatment is shown in Figure 26.

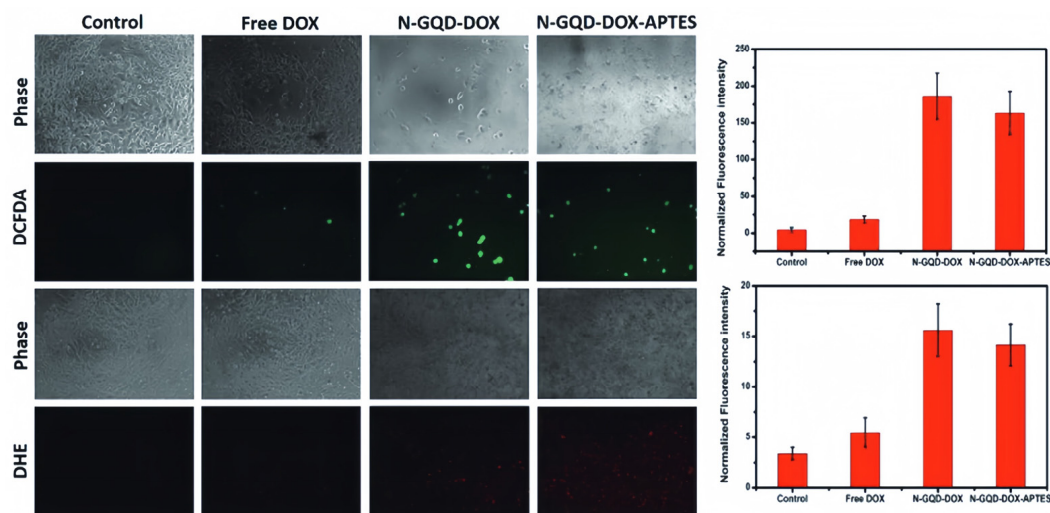


**Figure 26.** Tumor therapy-DOX, N-GQD-DOX, and N-GQD-DOX-APTES in MDA-MB-231 intracellular oxygen [142].

The working mechanism of photothermal therapy is to convert light energy into heat energy to kill tumors; specifically, when the light is irradiated, the electron absorption energy transitions from the ground state to the excited state, and the kinetic energy increases, making the surrounding environment hot [143]. Materials with photothermal conversion efficiency are transferred into the body and gathered around the tumor, using this method to kill tumor cells. Cao et al. [144] designed a quantum dot porphyrin derivative (GQD-PEG-P) with high unimodal oxygen production capacity and good optical performance that can be used for intracellular cancer-related microRNA detection of tumor cells, and the study found that the mortality rate of derivative-treated cells under laser irradiation was much higher than that of the control group, indicating that this method can be applied to removing cancer cells. Yao et al. [145] developed a system based on the Mesoporous silica nanoparticles as drug hydrochloride carriers and GQD as a local photoresist with a multi-functional synergistic chemical optical therapy platform. Experiments are performed to obtain this system, which has better cancer-removing ability than simple chemotherapy.

#### 6.4.2. Biological Imaging

Fluorescent molecules for bioimaging need to be bright and stable and easily bind to target molecules. Nowadays, fluorescent dyes have poor stability and often do not work well in many cases. GQDs have very good photoluminescence properties due to their nano-size, which, coupled with their low cytotoxicity, high biocompatibility, and photostability, has led to their attention as new fluorophores for bioimaging. The possibility of utilizing GQDs as fluorophores has been demonstrated by labeling multiple cell types [65]. Zhu et al. [23] reported a method of large-scale synthesis of GQDs with strong green fluorescent GQDs. The generated GQDs exhibited significant fluorescence with a fluorescence quantum yield of 11.4%. can be useful in bio-imaging as well as tracking. Jin et al. [146] synthesized S-GQDs using citric acid and sulfur powder as precursors, and S atoms were successfully introduced into the GQDs to diversify the paths of electron leaps, which improved the blue emission intensity of the GQDs, and the fluorescence intensity of the GQDs was significantly enhanced compared with that of the undoped GQDs, which resulted in an optimal emission wavelength of 460 nm at 380 nm, and the fluorescence response

performance of the doped quantum dots was utilized to more intuitively visualize the imaging content and to judgment. Zhang et al. [37] used a strong oxidant to treat graphite to obtain a GQDs of about 10 nm. It has good physiological solubility, high photostability, low cytotoxicity, and yellow-green fluorescence with a quantum yield of about 7%. Kuo et al. [147] prepared N-GQDs and compounded them with nitrogen-containing polymers. Presenting a wide range of colors from the UV to the NIR region with no spectral overlap allows for better applications in bio-imaging. Application in biological imaging is shown in Figure 27.

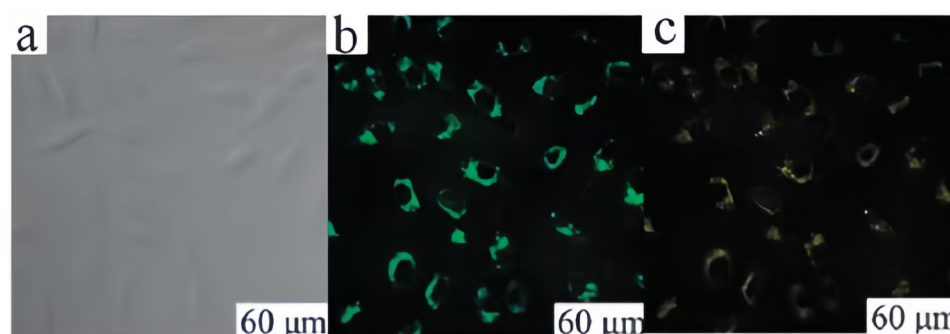


**Figure 27.** (a) Bright field image of MG-63 cells; (b) Image under 405 nm excitation; (c) image under 488 nm excitation [23].

Biosensors can also be fabricated using bioimaging technology for real-time monitoring of in vivo targets. The construction of multifunctional sensors with comprehensive diagnostic and dynamic real-time monitoring functions is one of the frontiers and hotspots of current research. Due to their large specific surface area and high photothermal conversion efficiency, GQDs can realize the loading and controlled release of drugs. The modifiable structure gives them the ability to target diseased tissues [148]. Zhao et al. [149] composited GQDs and o-phenylenediamine by stacking, where the o-phenylenediamine itself does not have fluorescence emission, and thus the composite exhibits the blue emission of GQDs. When  $\text{Ag}^+$  was detected by the probe, o-phenylenediamine was oxidized to produce 2,3-diaminophenazine with strong fluorescence emission at 557 nm, at which time there was a FRET process between GQDs and 2,3-diaminophenazine. Liu et al. [150] hydrothermally synthesized B,N-GQDs using graphite oxide, boric acid, and ammonia solution as raw materials and found that the excitation and emission spectra of the quantum dots completely overlapped with the absorption peaks in the UV-visible absorption spectra of  $\text{Hg}^{2+}$ , and thus the quenching of the fluorescence of the quantum dots by  $\text{Hg}^{2+}$  was due to the IFE fluorescence mechanism.

#### 6.4.3. Drug Delivery Systems

Because of its low toxicity and large specific surface area, graphene quantum dots have a great advantage in drug delivery. First, due to their size, they can easily pass through the loose vascular pores and stay at the tumor site to react, and second, due to their biocompatibility characteristics, they can interact stably with various molecules. Due to their smaller size, greater biocompatibility, easier cellular uptake, and cellular toxicity, they are considered a safe and effective drug delivery vehicle [151]. Drug delivery systems (DDS) load drugs into nanomaterials by adsorption or encapsulation to form drug nanoparticles [152]. Compared with free drug molecules, it has the very obvious advantage that it can enter tumor tissues through the lax vascular pores of tumor tissues, producing high penetration and retention effects at the tumor site. This system can not only realize the co-administration or targeted delivery of multiple drugs but also increase drug utilization, reduce side effects, prolong the circulating half-life, and improve the pharmacokinetics [153,154]. Wang et al. [155] prepared a stable DOX/GQD conjugate through the interaction of GQD and DOX. DOX/GQD conjugate can deliver DOX specifically into the nucleus, while GQD can also deliver DOX specifically into the nucleus. The

DOX/GQD conjugate can specifically deliver DOX into the nucleus, and GQD can also enhance the DNA cleavage activity of DOX. Increasing the cumulative concentration of DOX in the nucleus and enhancing the DNA cleavage activity can increase the cytotoxicity of drug-resistant cancer cells. Iannazzo et al. [156] developed a novel delivery system to selectively release therapeutic drugs into cancer cells. GQDs are covalently linked to biotin to recognize the biotin receptor overexpressed on tumor cells. Using the adsorption properties of carbon nanomaterials, the chemotherapeutic drug Adriamycin was loaded onto the surface of the GQDs, and the intrinsic fluorescence of Adriamycin could also be used to track drug release. In their experiments, they found that the cellular uptake of chemotherapeutic drugs gradually increased over time and reached a maximum after a few hours; subsequently, the uptake began to decrease again due to the increase in mortality. Sung et al. [157] prepared “nanosponges” by loading the GQDs and photosensitizing drugs onto porous silica and wrapping cetuximab-immobilized erythrocyte membranes around their surfaces. The tumor-targeting properties of cetuximab increased the aggregation of nanoparticles at the tumor site, and the heat generated by the nanosponges triggered the release of GQDs and drugs under near-infrared light irradiation, which effectively killed and inhibited the tumor.

## 7. The Challenges and Summary Prospects Faced

In summary, GQDs, as a new type of carbon nanomaterial, have great potential for development in various fields. Although GQDs have made significant progress, they still face challenges in some areas due to some unsolved problems. For example, the optical and electrical properties of GQDs are strongly dependent on their size and morphology, and the methods for synthesizing GQDs have drawbacks such as being time-consuming and environmentally harmful. Obtaining monolayers of GQDs with narrow size distributions that are high quality and precisely controllable is still a challenge. There is no clear boundary for the luminescence mechanism of GQDs, and there is no generalized model to explain all the photoluminescence properties of GQDs in a clear and detailed way, which severely limits the further increase of quantum yield. Optimization is also needed in terms of the detection of gas species, stability, and response performance. (1) adjusting the size of the GQDs during the preparation process, which in turn regulates their forbidden bandwidths and electron transfer efficiency, so as to enable the response performance of the gas sensors to be improved; (2) adopting chemical group modification and elemental doping to make the GQDs easy to bind with specific gases and improve the selectivity of the gas sensors; and (3) further exploring the compounding conditions of the GQDs with other gas-sensitive materials to improve the stability, high-temperature resistance, and aging resistance of the gas sensors. There are also many deficiencies in the study of the biological toxicity of GQDs. Most of the current studies on the biotoxicity of GQDs have ignored the potential phototoxicity of GQDs under light exposure, which generates reactive oxygen radicals under light excitation, which reduces cell activity and even leads to apoptosis. In the field of biological detection, there are still few studies on the simultaneous real-time monitoring of carriers and drug molecules in the process of tumor treatment, and more in-depth research is still needed to truly realize the accurate diagnosis and real-time monitoring of tumors. Therefore, the development of multifunctional GQD drug carriers with optical imaging of tumors, controllable drug release, and real-time monitoring of drug release remains a major challenge.

Although there are still many unsolved problems, its excellent optical properties, good biocompatibility, stable photoluminescence, and good solubility due to edge and quantum domain-limited effects are gradually becoming a hotspot in many research fields. The modified graphene quantum dots have the advantages of tunable photoluminescence and fluorescence stability and have broad application prospects in various fields such as biological imaging, fluorescence sensing, cancer treatment, and photocatalysis. In short, the research on GQDs is still in the exploratory stage, and with the deepening of exploration, GQDs as a new multifunctional material may be more widely used in many fields.

**Author Contributions:** Y.C. (Yibo Cui): Conceptualization, investigation, writing—original draft preparation. L.L.: Methodology. M.S.: Software. Y.W.: Validation. X.M.: Formal analysis. Y.C. (YanJun Chen): Data curation. Q.H.: Funding acquisition, visualization, writing—review and editing. C.L.: project administration, supervision. All authors have read and agreed to the published version of the manuscript.

**Funding:** This study has been sponsored by National Natural Science Foundation of China (12202410 and 51906238), Project funded by China Postdoctoral Science Foundation (2023T160734 and 2023M733935), Natural Science Foundation of Hunan Province (2023JJ40726), Research Project Supported by Shanxi Scholarship Council of China (2022-139), Supported by Fundamental Research Program of Shanxi Province (20210302123017, 202203021221120 and 202303021211145), Fund Program for the Scientific Activities of Selected Returned Overseas Professionals in Shanxi Province (20220012), Supported by the Opening Foundation of Key Laboratory in North University of China (DXMBJJ2023-03) and Changsha Municipal Natural Science Foundation (kq2208277). Also, the authors thank Wei Yue from Shiyanjia Lab (<https://www.shiyanjia.com>) for the SEM analysis.

**Data Availability Statement:** Data will be made available on request.

**Conflicts of Interest:** The authors declare no conflicts of interest.

## References

1. Liu, C.; Xu, D.; Weng, J.; Zhou, S.; Li, W.; Wan, Y.; Jiang, S.; Zhou, D.; Wang, J.; Huang, Q. Phase change materials application in battery thermal management system: A review. *Materials* **2020**, *13*, 4622. [[CrossRef](#)] [[PubMed](#)]
2. Novoselov, K.S.; Geim, A.K.; Morozov, S.V.; Jiang, D.; Zhang, Y.; Dubonos, S.; Grigorieva, I.V.; Firsov, A.A. Electric field effect in atomically thin carbon films. *Science* **2004**, *306*, 666–669. [[CrossRef](#)] [[PubMed](#)]
3. Lee, C.; Wei, X.; Kysar, J.W.; Hone, J. Measurement of the elastic properties and intrinsic strength of monolayer graphene. *Science* **2008**, *321*, 385–388. [[CrossRef](#)] [[PubMed](#)]
4. Nair, R.R.; Blake, P.; Grigorenko, A.N.; Novoselov, K.S.; Booth, T.J.; Stauber, T.; Peres, N.M.R.; Geim, A.K. Fine structure constant defines visual transparency of graphene. *Science* **2008**, *320*, 1308. [[CrossRef](#)] [[PubMed](#)]
5. Xie, R.; Wang, Z.; Zhou, W.; Liu, Y.; Fan, L.; Li, Y.; Li, X. Graphene quantum dots as a smart probe for biosensing. *Anal. Methods* **2016**, *8*, 4001–4016. [[CrossRef](#)]
6. Guin, S.K.; Ambolliker, A.S.; Guin, J.P.; Neogy, S. Exploring the excellent photophysical and electrochemical properties of graphene quantum dots for complementary sensing of uranium. *Sens. Actuators B Chem.* **2018**, *272*, 559–573. [[CrossRef](#)]
7. Zhu, S.; Zhang, J.; Tang, S.; Qiao, C.; Wang, L.; Wang, H.; Liu, X.; Li, B.; Li, Y.; Yu, W.; et al. Surface chemistry routes to modulate the photoluminescence of graphene quantum dots: From fluorescence mechanism to up-conversion bioimaging applications. *Adv. Funct. Mater.* **2012**, *22*, 4732–4740. [[CrossRef](#)]
8. Ha, M.; Kim, J.-H.; You, M.; Li, Q.; Fan, C.; Nam, J.-M. Multicomponent plasmonic nanoparticles: From heterostructured nanoparticles to colloidal composite nanostructures. *Chem. Rev.* **2019**, *119*, 12208–12278. [[CrossRef](#)]
9. Yan, X.; Li, B.; Cui, X.; Wei, Q.; Tajima, K.; Li, L.-S. Independent Tuning of the Band Gap and Redox Potential of Graphene Quantum Dots. *Phys. Chem. Lett.* **2011**, *2*, 1119. [[CrossRef](#)]
10. Liu, F.; Jang, M.-H.; Ha, H.D.; Kim, J.-H.; Cho, Y.-H.; Seo, T.S. Facile synthetic method for pristine graphene quantum dots and graphene oxide quantum dots: Origin of blue and green luminescence. *Adv. Mater.* **2013**, *25*, 3657–3662. [[CrossRef](#)]
11. Zheng, X.T.; Ananthanarayanan, A.; Luo, K.Q.; Chen, P. Glowing graphene quantum dots and carbon dots properties, syntheses, and biological applications. *Small* **2015**, *11*, 1620–1636. [[CrossRef](#)] [[PubMed](#)]
12. Dong, S.; Yuan, Z.; Zhang, L.; Lin, Y.; Lu, C. Rapid screening of oxygen states in carbon quantum dots by chemiluminescence probe. *Anal. Chem.* **2017**, *89*, 12520–12526. [[CrossRef](#)] [[PubMed](#)]
13. Meng, Z.; Stolz, R.M.; Mendecki, L.; Mirica, K.A. Electrically-transduced chemical sensors based on two-dimensional nanomaterials. *Chem. Rev.* **2019**, *119*, 478–598. [[CrossRef](#)] [[PubMed](#)]
14. Liu, M.L.; Chen, B.B.; Li, C.M.; Huang, C.Z. Carbon dots: Synthesis, formation mechanism, fluorescence origin and sensing applications. *Green. Chem.* **2019**, *21*, 449–471. [[CrossRef](#)]
15. Bai, H.; Shi, G. Gas Sensors Based on Conducting Polymers. *Sensors* **2007**, *7*, 267–307. [[CrossRef](#)]
16. Chen, W.; Li, F.; Ooi, P.C.; Ye, Y.; Kim, T.W.; Guo, T. Room temperature pH-dependent ammonia gas sensors using graphene quantum dots. *Sens. Actuators B* **2016**, *222*, 763–768. [[CrossRef](#)]
17. Orecchioni, M.; Menard-Moyon, C.; Delogu, L.G.; Bianco, A. Graphene and the immune system: challenges and potentiality. *Adv. Drug Deliv. Rev.* **2016**, *105 Pt B*, 163–175. [[CrossRef](#)]
18. Shen, J.; Zhu, Y.; Yang, X.; Li, C. ChemInform Abstract: Graphene Quantum Dots: Emergent Nanolights for Bioimaging, Sensors, Catalysis and Photovoltaic Devices. *Chem. Commun.* **2012**, *48*, 3686. [[CrossRef](#)]
19. Coluci, V.R.; Galvao, D.S.; Baughman, R.H. Theoretical investigation of electromechanical effects for graphyne carbon nanotubes. *J. Chem. Phys.* **2004**, *121*, 3228–3237. [[CrossRef](#)]
20. Geim, A.K.; MacDonald, A.H. Graphene: Exploring carbon flatland. *Phys. Today* **2007**, *60*, 35–41. [[CrossRef](#)]

21. Baker, S.N.; Baker, G.A. Luminescent carbon nanodots emergent nanolights. *Angew. Chem. Int. Ed. Engl.* **2010**, *49*, 6726–6744. [[CrossRef](#)]
22. Li, L.; Wu, G.; Yang, G.; Peng, J.; Zhao, J.; Zhu, J.-J. Focusing on luminescent graphene quantum dots: Current status and future perspectives. *Nanoscale* **2013**, *5*, 4015–4039. [[CrossRef](#)] [[PubMed](#)]
23. Zhu, S.; Zhang, J.; Qiao, C.; Tang, S.; Li, Y.; Yuan, W.; Li, B.; Tian, L.; Liu, F.; Hu, R.; et al. Strongly green-photoluminescent graphene quantum dots for bioimaging. *Chem. Commun.* **2011**, *47*, 6858–6860. [[CrossRef](#)]
24. Li, H.; He, X.; Kang, Z.; Huang, H.; Liu, Y.; Liu, J.; Lian, S.; Tsang, C.H.A.; Yang, X.; Lee, S.-T. Water-soluble fluorescent carbon quantum dots and photocatalyst design. *Angew. Chem. Int. Ed. Engl.* **2010**, *49*, 4430–4434. [[CrossRef](#)] [[PubMed](#)]
25. Cho, H.-H.; Yang, H.; Kang, D.J.; Kim, B.J. Surface engineering of graphene quantum dots and their applications as efficient surfactants. *ACS Appl. Mater. Interfaces* **2015**, *7*, 8615–8621. [[CrossRef](#)] [[PubMed](#)]
26. Dong, Y.; Tian, W.; Ren, S.; Dai, R.; Chi, Y.; Chen, G. Graphene quantum dots/L-cysteine coreactant electrochemiluminescence system and its application in sensing lead(ii) ions. *ACS Appl. Mater. Interfaces* **2014**, *6*, 1646–1651. [[CrossRef](#)] [[PubMed](#)]
27. Gao, Y.; Tian, E.; Zhang, Y.; Mo, J. Utilizing electrostatic effect in fibrous filters for efficient airborne particles removal: Principles, fabrication, and material properties. *ScienceDirect* **2022**, *03*, 101369. [[CrossRef](#)]
28. Chong, Y.; Ma, Y.; Shen, H.; Tu, X.; Zhou, X.; Xu, J.; Dai, J.; Fan, S.; Zhang, Z. The in vitro and in vivo toxicity of graphene quantum dots. *Biomaterials* **2014**, *35*, 5041–5048. [[CrossRef](#)]
29. Iravani, S.; Varma, R.S. Green synthesis, biomedical and biotechnological applications of carbon and graphene quantum dots. A review. *Environ. Chem. Lett.* **2020**, *18*, 703–727. [[CrossRef](#)]
30. Perini, G.; Palmieri, V.; Ciasca, G.; De Spirito, M.; Papi, M. Unravelling the Potential of Graphene Quantum Dots in Biomedicine and Neuroscience. *Int. J. Mol. Sci.* **2020**, *21*, 3712. [[CrossRef](#)]
31. Zhu, J.; Tang, Y.; Wang, G.; Mao, J.; Liu, Z.; Sun, T.; Wang, M.; Chen, D.; Yang, Y.; Li, J.; et al. Green, rapid, and universal preparation approach of graphene quantum dots under ultraviolet irradiation. *ACS Appl. Mater. Interfaces* **2017**, *9*, 14470–14477. [[CrossRef](#)] [[PubMed](#)]
32. Lu, J.; Yang, J.-X.; Wang, J.; Lim, A.; Wang, S.; Loh, K.P. One-Pot Synthesis of Fluorescent Carbon Nanoribbons, Nanoparticles, and Graphene by the Exfoliation of Graphite in Ionic Liquids. *ACS Nano* **2009**, *3*, 367–2375. [[CrossRef](#)]
33. Li, X.; Wang, H.; Shimizu, Y.; Pyatenko, A.; Kawaguchi, K.; Koshizaki, N. Preparation of carbon quantum dots with tunable photoluminescence by rapid laser passivation in ordinary organic solvents. *Chem. Commun.* **2010**, *47*, 932–934. [[CrossRef](#)] [[PubMed](#)]
34. Zhang, Y.; Yang, X.; Pu, Y.; Cheng, W.; Lin, S.; Shao, Z.; Liao, X. Selective, sensitive and label-free detection of Fe<sup>3+</sup> ion in tap water using highly fluorescent graphene quantum dots. *J. Fluoresc.* **2019**, *29*, 541–548. [[CrossRef](#)]
35. Wang, Y.; Wu, W.-T.; Wu, M.-B.; Sun, H.-D.; Xie, H.; Hu, C.; Wang, X.-N.; Wu, X.-Y.; Qiu, J.-S. Yellow-visual fluorescent carbon quantum dots from petroleum coke for the efficient detection of Cu<sup>2+</sup> ions. *New Carbon Mater.* **2016**, *6*, 550–559. [[CrossRef](#)]
36. Pan, D.; Zhang, J.; Li, Z.; Wu, M. Hydrothermal route for cutting graphene sheets into blue-luminescent graphene quantum dots. *Adv. Mater.* **2010**, *22*, 734–738. [[CrossRef](#)] [[PubMed](#)]
37. Zhang, L.; Xing, Y.; He, N.; Zhang, Y.; Lu, Z.; Zhang, J.; Zhang, Z. Preparation of graphene quantum dots for bioimaging application. *J. Nanosci. Nanotechnol.* **2012**, *12*, 2924–2948. [[CrossRef](#)]
38. Peng, J.; Gao, W.; Gupta, B.K.; Liu, Z.; Romero-Aburto, R.; Ge, L.; Song, L.; Alemany, L.B.; Zhan, X.; Gao, G.; et al. Graphene Quantum Dots Derived from Carbon Fibers. *Nano Lett.* **2012**, *12*, 844. [[CrossRef](#)]
39. Li, L.-L.; Ji, J.; Fei, R.; Wang, C.-Z.; Lu, Q.; Zhang, J.-R.; Jiang, L.-P.; Zhu, J.-J. A facile microwave avenue to electrochemiluminescent two-color graphene quantum dots. *Adv. Funct. Mater.* **2012**, *22*, 2971–2979. [[CrossRef](#)]
40. Luo, Z.; Qi, G.; Chen, K.; Zou, M.; Yuwen, L.; Zhang, X.; Huang, W.; Wang, L. Microwave-assisted preparation of white fluorescent graphene quantum dots as a novel phosphor for enhanced white-light-emitting diodes. *Adv. Funct. Mater.* **2016**, *26*, 2739–2744. [[CrossRef](#)]
41. Zhuo, S.; Shao, M.; Lee, S.-T. Upconversion and downconversion fluorescent graphene quantum dots: Ultrasonic preparation and photocatalysis. *ACS Nano* **2012**, *6*, 1059–1064. [[CrossRef](#)] [[PubMed](#)]
42. Lu, J.; Yeo, P.S.E.; Gan, C.K.; Wu, P.; Loh, K.P. Transforming C60 molecules into graphene quantum dots. *Nat. Nanotechnol.* **2011**, *6*, 247–252. [[CrossRef](#)] [[PubMed](#)]
43. Zhou, S.; Xu, H.; Gan, W.; Yuan, Q. Graphene quantum dots: Recent progress in preparation and fluorescence sensing applications. *RSC Adv.* **2016**, *6*, 110775–110788. [[CrossRef](#)]
44. Yan, X.; Cui, X.; Li, L.-S. Synthesis of Large, Stable Colloidal Graphene Quantum Dots with Tunable. *J. Am. Chem. Soc.* **2010**, *132*, 5944. [[CrossRef](#)] [[PubMed](#)]
45. Tang, L.; Ji, R.; Li, X.; Teng, K.S.; Lau, S.P. Size-Dependent Structural and Optical Characteristics of Glucose-Derived Graphene Quantum Dots. *Part. Part. Syst. Character.* **2013**, *30*, 523–531. [[CrossRef](#)]
46. Huang, H.; Yang, S.; Li, Q.; Yang, Y.; Wang, G.; You, X.; Mao, B.; Wang, H.; Ma, Y.; He, P.; et al. Electrochemical cutting in weak aqueous electrolyte: The strategy for efficient and controllable preparation of graphene quantum dots. *Langmuir* **2018**, *34*, 250–258. [[CrossRef](#)] [[PubMed](#)]
47. Tan, X.; Li, Y.; Li, X.; Zhou, S.; Fan, L.; Yang, S. Electrochemical synthesis of small-sized red fluorescent graphene quantum dots as a bioimaging platform. *Chem. Commun.* **2015**, *51*, 2544–2546. [[CrossRef](#)]

48. Wongrat, E.; Nuengnit, T.; Panyathip, R.; Chanlek, N.; Hongsith, N.; Choopun, S. Highly Selective Room Temperature Ammonia Sensors Based on ZnO Nanostructures Decorated with Graphene Quantum Dots (GQDs). *Sens. Actuators B* **2021**, *326*, 128983. [[CrossRef](#)]
49. Su, J.; Zhang, X.; Tong, X.; Wang, X.; Yang, P.; Yao, F.; Guo, R.; Yuan, C. Preparation of graphene quantum dots with high quantum yield by a facile one-step method and applications for cell imaging. *Mater. Lett.* **2020**, *271*, 127806. [[CrossRef](#)]
50. Shen, J.; Zhu, Y.; Yang, X.; Zong, J.; Zhang, J.; Li, C. One-pot hydrothermal synthesis of graphene quantum dots surface-passivated by polyethylene glycol and their photoelectric conversion under near-infrared light. *New J. Chem* **2012**, *36*, 97–101. [[CrossRef](#)]
51. Pan, D.; Guo, L.; Zhang, J.; Xi, C.; Xue, Q.; Huang, H.; Li, J.; Zhang, Z.; Yu, W.; Chen, Z.; et al. Cutting sp<sup>2</sup> clusters in graphene sheets into colloidal graphene quantum dots with strong green fluorescence. *Mater. Chem.* **2012**, *22*, 3314–3318. [[CrossRef](#)]
52. Shen, J.; Zhu, Y.; Chen, C.; Yang, X.; Li, C. Facile preparation and upconversion luminescence of graphene quantum dots. *Chem. Commun.* **2011**, *47*, 2580. [[CrossRef](#)] [[PubMed](#)]
53. Chen, Y.; Xie, Y.; Yan, X.; Cohen, M.L.; Zhang, S. Topological carbon materials: A new perspective. *Phys. Rep.* **2020**, *868*, 1–32. [[CrossRef](#)]
54. Lu, Q.; Wu, C.; Liu, D.; Wang, H.; Su, W.; Li, H.; Zhang, Y.; Yao, S. A facile and simple method for synthesis of graphene oxide quantum dots from black carbon. *Green Chem.* **2017**, *19*, 900–904. [[CrossRef](#)]
55. Chen, W.; Lv, G.; Hu, W.; Li, D.; Chen, S.; Dai, Z. Synthesis and applications of graphene quantum dots: A review. *Nanotechnol. Rev.* **2017**, *7*, 157–185. [[CrossRef](#)]
56. Shehab, M.; Ebrahim, S.; Soliman, M. Graphene quantum dots prepared from glucose as optical sensor for glucose. *Lumin* **2017**, *184*, 110–116. [[CrossRef](#)]
57. Qu, D.; Sun, Z.; Zheng, M.; Li, J.; Zhang, Y.; Zhang, G.; Zhao, H.; Liu, X.; Xie, Z. Three colors emission from n co-doped graphene quantum dots for visible light H<sub>2</sub> production and bioimaging. *Adv. Opt. Mater.* **2015**, *3*, 360–367. [[CrossRef](#)]
58. Liu, R.; Wu, D.; Feng, X.; Mülle, K. Bottom-Up Fabrication of Photoluminescent Graphene Quantum Dots with Uniform Morphology. *J. Am. Chem. Soc.* **2011**, *133*, 15221–15223. [[CrossRef](#)]
59. Kaciulis, S.; Mezzi, A.; Soltani, P.; Pizzoferrato, R.; Ciotta, E.; Proposito, P. Graphene quantum dots obtained by unfolding fullerene. *Thin Solid Film.* **2019**, *673*, 19–25. [[CrossRef](#)]
60. Fan, L.; Zhu, M.; Lee, X.; Zhang, R.; Wang, K.; Wei, J.; Zhong, M.; Wu, D.; Zhu, H. Direct synthesis of graphene quantum dots by chemical vapor deposition. *Part. Part. Syst. Character.* **2013**, *30*, 764–769. [[CrossRef](#)]
61. Lee, J.; Kim, K.; Park, W.I.; Kim, B.-H.; Park, J.H.; Kim, T.-H.; Bong, S.; Kim, C.-H.; Chae, G.; Jun, M.; et al. Uniform Graphene Quantum Dots Patterned from Self-Assembled Silica Nanodots. *Nano Lett.* **2012**, *12*, 6078–6083. [[CrossRef](#)] [[PubMed](#)]
62. Wang, L.; Li, W.; Wu, B.; Li, Z.; Wang, S.; Liu, Y.; Pan, D.; Wu, M. Facile synthesis of fluorescent graphene quantum dots from coffee grounds for bioimaging and sensing. *Chem. Eng. J.* **2016**, *300*, 75–82. [[CrossRef](#)]
63. Ding, Z.; Li, F.; Wen, J.; Wang, X.; Sun, R. Gram-scale synthesis of single-crystalline graphene quantum dots derived from lignin biomass. *Green. Chem.* **2018**, *20*, 1383–1390. [[CrossRef](#)]
64. Tran, H.L.; Darmanto, W.; Doong, R.-A. Ultrasensitive detection of tetracycline using boron and nitrogen codoped graphene quantum dots from natural carbon source as the paper-based nanosensing probe in difference matrices. *Nanomaterials* **2020**, *10*, 1883. [[CrossRef](#)] [[PubMed](#)]
65. Kalluri, A.; Dharmadhikari, B.; Debnath, D.; Patra, P.; Kumar, C.V. Advances in Structural Modifications and Properties of Graphene Quantum Dots for Biomedical Applications. *ACS Omega* **2023**, *6*, 21358–21376. [[CrossRef](#)] [[PubMed](#)]
66. Feng, Q.; Cao, Q.; Li, M.; Liu, F.; Tang, N.; Du, Y. Synthesis and photoluminescence of fluorinated graphene quantum dots. *Appl. Phys. Lett.* **2013**, *102*, 013111. [[CrossRef](#)]
67. Fu, J.; Wang, Y.; Liu, J.; Huang, K.; Chen, Y.; Li, Y.; Zhu, J.-J. Low overpotential for electrochemically reducing CO<sub>2</sub> to CO on nitrogen-doped graphene quantum dots-wrapped single-crystalline gold nanoparticles. *ACS Energy Lett.* **2018**, *3*, 946–951. [[CrossRef](#)]
68. Wang, H.; Revia, R.; Mu, Q.; Lin, G.; Yen, C.; Zhang, M. Single-layer borondoped graphene quantum dots for contrast-enhanced in vivo T1-weighted MRI. *Nanoscale Horiz.* **2020**, *5*, 573–579. [[CrossRef](#)]
69. Ganganboina, A.B.; Dega, N.K.; Tran, H.L.; Darmonto, W.; Doong, R.-A. Application of sulfur-doped graphene quantum dots@gold-carbon nanosphere for electrical pulse-induced impedimetric detection of glioma cells. *Biosens. Bioelectron.* **2021**, *181*, 113151. [[CrossRef](#)]
70. Wang, H.; Mu, Q.; Wang, K.; Revia, R.A.; Yen, C.; Gu, X.; Tian, B.; Liu, J.; Zhang, M. Nitrogen and borondual-doped graphene quantum dots for near-infrared second window imaging and photothermal therapy. *Appl. Mater. Today* **2019**, *14*, 108117. [[CrossRef](#)]
71. Kumara, B.N.; Kalimuthu, P.; Prasad, K.S. Synthesis, properties and potential applications of photoluminescent carbon nanoparticles: A review. *Anal. Chim. Acta* **2023**, *1268*, 341430. [[CrossRef](#)]
72. Wu, W.; Zhan, L.; Fan, W.; Song, J.; Li, X.; Li, Z.; Wang, R.; Zhang, J.; Zheng, J.; Wu, M.; et al. Cu-N dopants boost electron transfer and photooxidation reactions of carbon dots. *Angew. Chem.* **2015**, *54*, 6540–6544. [[CrossRef](#)] [[PubMed](#)]
73. Zhang, Q.; Xu, W.; Han, C.; Wang, X.; Wang, Y.; Li, Z.; Wu, W.; Wu, M. Graphene structure boosts electron transfer of dual-metal doped carbon dots in photooxidation. *Carbon* **2018**, *126*, 128–134. [[CrossRef](#)]
74. Zhang, J.; Ma, Y.-Q.; Li, N.; Zhu, J.-L.; Zhang, T.; Zhang, W.; Liu, B. Preparation of graphene quantum dots and their application in cell imaging. *J. Nanomater.* **2016**, *2016*, 9245865. [[CrossRef](#)]

75. Calabro, R.L.; Yang, D.-S.; Kim, D.Y. Controlled nitrogen doping of graphene quantum dots through laser ablation in aqueous solutions for photoluminescence and electrocatalytic applications. *ACS Appl. Nano Mater.* **2019**, *2*, 6948–6959. [[CrossRef](#)]
76. Xin, Q.; Shah, H.; Xie, W.; Wang, Y.; Jia, X.; Nawaz, A.; Song, M.; Gong, J.R. Preparation of blue- and green-emissive nitrogen-doped graphene quantum dots from graphite and their application in bioimaging. *Mater. Sci. Eng. C* **2021**, *119*, 11164. [[CrossRef](#)]
77. Qu, D.; Zheng, M.; Peng, D.; Zhou, Y.; Zhang, L.; Li, D.; Tan, H.; Zhao, Z.; Xie, Z.; Sun, Z. Highly luminescent S, N co-doped graphene quantum dots with broad visible absorption bands for visible light photocatalysts. *Nanoscale* **2013**, *5*, 12272–12277. [[CrossRef](#)] [[PubMed](#)]
78. Yan, Z.; Qu, X.; Niu, Q.; Tian, C.; Fan, C.; Ye, B. A green synthesis of highly fluorescent nitrogen-doped graphene quantum dots for the highly sensitive and selective detection of mercury(II) ions and biothiols. *Anal. Methods* **2016**, *8*, 1565–1571. [[CrossRef](#)]
79. Benitez-Martinez, S.; Lopez-Lorente, A.I.; Valcarcel, M. Determination of TiO<sub>2</sub> nanoparticles in sunscreen using N-doped graphene quantum dots as a fluorescent probe. *Microchim. Acta* **2016**, *183*, 781–789. [[CrossRef](#)]
80. Yang, Y.; Gu, B.; Liu, Z.; Chen, D.; Zhao, Y.; Guo, Q.; Wang, G. Hydrothermal synthesis of N, P co-doped graphene quantum dots for high-performance Fe<sup>3+</sup> detection and bioimaging. *J. Nanopart. Res.* **2021**, *23*, 40. [[CrossRef](#)]
81. Li, Y.; Li, S.; Wang, Y.; Wang, J.; Liu, X.; Wang, L.; Liu, X.; Xue, W.; Ma, N. Electrochemical synthesis of phosphorus doped graphene quantum dots for free radical scavenging. *Phys. Chem. Chem. Phys.* **2017**, *19*, 11631–11638. [[CrossRef](#)]
82. Wang, W.; Xu, S.; Li, N.; Huang, Z.; Su, B.; Chen, X. Sulfur and phosphorus codoped graphene quantum dots for fluorescent monitoring of nitrite in pickles. *Spectrochim. Acta Part. A Mol. Biomol. Spectrosc.* **2019**, *221*, 117211. [[CrossRef](#)] [[PubMed](#)]
83. Qian, J.; Shen, C.; Yan, J.; Xi, F.; Dong, X.; Liu, J. Tailoring the electronic properties of graphene quantum dots by P doping and its enhanced performance in metal-free composite photocatalyst. *J. Phys. Chem. C* **2018**, *122*, 349–358. [[CrossRef](#)]
84. Fan, T.; Zhang, G.; Jian, L.; Murtaza, I.; Meng, H.; Liu, Y.; Min, Y. Facile synthesis of defect-rich nitrogen and sulfur co-doped graphene quantum dots as metal-free electrocatalyst for the oxygen reduction reaction. *J. Alloys Compd.* **2019**, *792*, 844–850. [[CrossRef](#)]
85. Yang, L.; Wei, J.; Ma, Z.; Song, P.; Ma, J.; Zhao, Y.; Huang, Z.; Zhang, M.; Yang, F. The fabrication of micro/nano structures by laser machining. *Nanomaterials* **2019**, *9*, 1789. [[CrossRef](#)] [[PubMed](#)]
86. Luo, Y.; Li, M.; Sun, L.; Xu, Y.; Li, M.; Hu, G.; Tang, T.; Wen, J.; Li, X.; Zhang, J.; et al. High fluorescent sulfur regulating graphene quantum dots with tunable photoluminescence properties. *J. Colloid Interface Sci.* **2018**, *529*, 205–213. [[CrossRef](#)] [[PubMed](#)]
87. Hasan, M.T.; Gonzalez-Rodriguez, R.; Ryan, C.; Faerber, N.; Cofffer, J.L.; Anton; Naumov, V. Photo- and electroluminescence from nitrogen-doped and nitrogensulfur codoped graphene quantum dots. *Adv. Funct. Mater.* **2018**, *28*, 1804337. [[CrossRef](#)]
88. Luo, Y.; Li, M.; Hu, G.; Tang, T.; Wen, J.; Li, X.; Wang, L. Enhanced photocatalytic activity of sulfur-doped graphene quantum dots decorated with TiO<sub>2</sub> nanocomposites. *Mater. Res. Bull.* **2018**, *97*, 428–435. [[CrossRef](#)]
89. Yang, Z.; Yao, Z.; Li, G.; Fang, G.; Nie, H.; Liu, Z.; Zhou, X.; Chen, X.; Huang, S. Sulfur-doped graphene as an efficient metal-free cathode catalyst for oxygen reduction. *ACS Nano* **2012**, *6*, 205–211. [[CrossRef](#)]
90. Ge, S.; He, J.; Ma, C.; Liu, J.; Xi, F.; Dong, X. One-step synthesis of boron-doped graphene quantum dots for fluorescent sensors and biosensor. *Talanta* **2019**, *199*, 581–589. [[CrossRef](#)]
91. Zhang, L.; Zhang, Z.-Y.; Liang, R.-P.; Li, Y.-H.; Qiu, J.-D. Boron-doped graphene quantum dots for selective glucose sensing based on the “abnormal” aggregation-induced photoluminescence enhancement. *Anal. Chem.* **2014**, *86*, 4423–4430. [[CrossRef](#)] [[PubMed](#)]
92. Xu, Y.; Wang, S.; Hou, X.; Sun, Z.; Jiang, Y.; Dong, Z.; Tao, Q.; Man, J.; Cao, Y. Coal-derived nitrogen, phosphorus and sulfur co-doped graphene quantum dots: A promising ion fluorescent probe. *Appl. Surf. Sci.* **2018**, *445*, 519–526. [[CrossRef](#)]
93. Islam, M.S.; Deng, Y.; Tong, L.; Roy, A.K.; Faisal, S.N.; Hassan, M.; Minnett, A.I.; Gomes, V.G. In-situ direct grafting of graphene quantum dots onto carbon fibre by low temperature chemical synthesis for high performance flexible fabric supercapacitor. *Mater. Today Commun.* **2016**, *10*, 112–119. [[CrossRef](#)]
94. Kang, S.-Y.; Yin, H.; Zhang, K.-Q.; Chen, X.; Wang, K.-Z. Chemosensing properties and logic gate behaviors of graphene quantum dot appended terpyridine. *Mater. Sci. Eng. C* **2019**, *99*, 657–668. [[CrossRef](#)] [[PubMed](#)]
95. Pourhashem, S.; Ghasemy, E.; Rashidi, A.; Vaezi, M.R. Corrosion protection properties of novel epoxy nanocomposite coatings containing silane functionalized graphene quantum dots. *J. Alloys Compd.* **2018**, *731*, 1112–1118. [[CrossRef](#)]
96. Zhang, R.; Shen, W.; Zhong, M.; Zhang, J.; Guo, S. Carbon nanofibers cross-linked and decorated with graphene quantum dots as binder-free electrodes for flexible supercapacitors. *J. Phys. Chem. C* **2021**, *125*, 143–151. [[CrossRef](#)]
97. Chan, D.K.L.; Cheung, P.L.; Yu, J.C. A visible-light-driven composite photocatalyst of TiO<sub>2</sub> nanotube arrays and graphene quantum dots. *Beilstein J. Nanotechnol.* **2014**, *5*, 689–695. [[CrossRef](#)]
98. Tachi, S.; Morita, H.; Takahashi, M.; Okabayashi, Y.; Hosokai, T.; Sugai, T.; Kuwahara, S. Quantum yield enhancement in graphene quantum dots via esterification with benzyl alcohol. *Sci. Rep.* **2019**, *9*, 14115. [[CrossRef](#)]
99. Luo, P.; Guan, X.; Yu, Y.; Li, X. 4-Methoxyphenyl grafted onto graphene quantum dots surface via diazonium chemistry method. *Opt. Quantum Electron.* **2018**, *50*, 269. [[CrossRef](#)]
100. Wang, Y.; Liu, X.; Kong, W.; Wang, L.; Li, Y. Post-epoxidation of graphene quantum dots. *Chem. Phys. Lett.* **2018**, *706*, 140–144. [[CrossRef](#)]
101. Hossain, Z.; Shimizu, N. In Situ functionalization of graphene with reactive end group through amine diazotization. *J. Phys. Chem. C* **2017**, *121*, 25223–25228. [[CrossRef](#)]
102. Ge, Q.; Kong, W.-H.; Liu, X.-Q.; Wang, Y.-M.; Wang, L.-F.; Ma, N.; Li, Y. Hydroxylated graphene quantum dots as fluorescent probes for sensitive detection of metal ions. *Int. J. Miner. Metall. Mater.* **2020**, *27*, 91–99. [[CrossRef](#)]

103. Ashraf, G.; Asif, M.; Aziz, A.; Dao, A.Q.; Zhang, T.; Iftikhar, T.; Wang, Q.; Liu, H. Facet-energy inspired metal oxide extended hexapods decorated with graphene quantum dots: Sensitive detection of bisphenol A in live cells. *Nanoscale* **2020**, *12*, 9014–9023. [[CrossRef](#)]
104. Tian, P.; Tang, L.; Teng, K.; Lau, S. Graphene quantum dots from chemistry to applications. *Mater. Today Chem.* **2018**, *10*, 221–258. [[CrossRef](#)]
105. He, R.; Chen, R.; Luo, J.; Zhang, S.; Xu, D. Fabrication of graphene quantum dots modified BiOI/PAN flexible fiber with enhanced photocatalytic activity. *Acta Phys. Chim. Sin.* **2021**, *37*, 2011022. [[CrossRef](#)]
106. Zhang, J.; Zhang, F.; Yang, Y.; Guo, S.; Zhang, J. Composites of graphene quantum dots and reduced graphene oxide as catalysts for nitroarene reduction. *ACS Omega* **2017**, *2*, 7293–7298. [[CrossRef](#)]
107. Lalit, G.; Neha, A.; Rajni, V.; Bishnoi, S.; Husale, S.; Pandey, R.; Gupta, G. Graphene quantum dot-sensitized ZnO-nanorod/GaN-nanotower heterostructure-based high-performance UV photodetectors. *ACS Appl. Mater. Interfaces* **2020**, *12*, 47038–47047. [[CrossRef](#)]
108. Yang, H.; Wang, P.; Wang, D.; Zhu, Y.; Xie, K.; Zhao, X.; Yang, J.; Wang, X. New understanding on photocatalytic mechanism of Nitrogen-doped graphene quantum dots-decorated BiVO<sub>4</sub> nanojunction photocatalysts. *ACS Omega* **2017**, *2*, 3766–3773. [[CrossRef](#)]
109. Li, F.; Li, M.; Luo, Y.; Li, M.; Li, X.; Zhang, J.; Wang, L. The synergistic effect of pyridinic nitrogen and graphitic nitrogen of nitrogen-doped graphene quantum dots for enhanced TiO<sub>2</sub> nanocomposites photocatalytic performance. *Catalysts* **2018**, *8*, 438–449. [[CrossRef](#)]
110. Li, K.; Ji, M.; Chen, R.; Jiang, Q.; Xia, J.; Li, H. Construction of nitrogen and phosphorus co-doped graphene quantum dots/Bi<sub>5</sub>O<sub>7</sub> I composites for accelerated charge separation and enhanced photocatalytic degradation performance. *Chin. J. Catal.* **2020**, *41*, 1230–1239. [[CrossRef](#)]
111. Cai, A.; Wang, Q.; Chang, Y.; Wang, X. Graphitic carbon nitride decorated with S, N co-doped graphene quantum dots for enhanced visible-light-driven photocatalysis. *J. Alloys Compd.* **2017**, *692*, 189–193. [[CrossRef](#)]
112. Tian, H.; Shen, K.; Hu, X.; Qiao, L.; Zheng, W. N, S co-doped graphene quantum dots-graphene-TiO<sub>2</sub> nanotubes composite with enhanced photocatalytic activity. *J. Alloys Compd.* **2017**, *691*, 369–377. [[CrossRef](#)]
113. Li, N.; Than, A.; Wang, X.; Xu, S.; Sun, L.; Duan, H.; Xu, C.; Chen, P. Ultrasensitive profiling of metabolites using tyramine-functionalized graphene quantum dots. *ACS Nano* **2016**, *10*, 3622–3629. [[CrossRef](#)] [[PubMed](#)]
114. Liu, X.; Zhou, Z.; Wang, T.; Ma, C.; Yan, Y. N-doped graphene quantum dots for enhancing multi-level Bi<sub>2</sub>Ti<sub>2</sub>O<sub>7</sub> spheres photocatalytic activity via electronic trapping. *J. Dispers. Sci. Technol.* **2022**, *43*, 639–648. [[CrossRef](#)]
115. Zhu, M.Y.; Liu, Q.; Chen, W.; Yin, Y.; Ge, L.; Li, H.; Wang, K. Boosting the visible-light photoactivity of BiOCl/BiVO<sub>4</sub>/N-GQDs ternary hetero-junctions based on internal Z-scheme charge transfer of N-GQDs: Simultaneous band gap narrowing and carrier lifetime prolonging. *ACS Appl. Mater. Interfaces* **2017**, *9*, 38832–38841. [[CrossRef](#)]
116. Li, Y.; Zhao, Y.; Cheng, H.H.; Hu, Y.; Shi, G.Q.; Dai, L.; Qu, L.T. Nitrogen-Doped Graphene Quantum Dots with Oxygen-Rich Functional Groups. *J. Am. Chem. Soc.* **2012**, *134*, 15–18. [[CrossRef](#)]
117. Li, Y.; Hu, Y.; Zhao, Y.; Shi, G.Q.; Deng, L.; Hou, Y.B.; Qu, L.T. An Electrochemical Avenue to Green-Luminescent Graphene Quantum Dots as Potential Electron-Acceptors for Photovoltaics. *Adv. Mater.* **2011**, *23*, 776. [[CrossRef](#)]
118. Gupta, V.; Chaudhary, N.; Srivastava, R.; Sharma, G.D.; Bhardwaj, R.; Chand, S. Luminescent Graphene Quantum Dots for Organic Photovoltaic Devices. *J. Am. Chem. Soc.* **2011**, *133*, 9960–9963. [[CrossRef](#)]
119. Zhao, J.; Chen, G.; Zhu, L.; Li, G. Graphene quantum dots-based platform for the fabrication of electrochemical biosensors. *Electrochem. Commun.* **2011**, *13*, 31–33. [[CrossRef](#)]
120. Ran, Z.; Yang, H.; Li, Z.; Wang, K.; Zhao, J.; Ran, X.; Du, G.; Yang, L. Pillar[6]arene@AuNPs functionalized N-CQDs@Co<sub>3</sub>O<sub>4</sub> hybrid composite for ultrasensitive electrochemical detection of human epididymis protein 4. *ACS Sustain. Chem. Eng.* **2020**, *8*, 10161–10172. [[CrossRef](#)]
121. Zhang, P.; Zhuo, Y.; Chang, Y.; Yuan, R.; Chai, Y. Electrochemiluminescent graphene quantum dots as a sensing platform: A dual amplification for microRNA assay. *Anal. Chem.* **2015**, *87*, 10385–10391. [[CrossRef](#)]
122. Wang, M.; Yin, H.; Zhou, Y.; Meng, X.; Waterhouse, G.I.N.; Ai, S. A novel photoelectrochemical biosensor for the sensitive detection of dual microRNAs using molybdenum carbide nanotubes as nanocarriers and energy transfer between CQDs and AuNPs. *Chem. Eng. J.* **2019**, *365*, 351–357. [[CrossRef](#)]
123. Chen, Y.; Dong, Y.; Wu, H.; Chen, C.; Chi, Y.; Chen, G. Electrochemiluminescence sensor for hexavalent chromium based on the graphene quantum dots/peroxodisulfate system. *Electrochim. Acta* **2015**, *151*, 552–557. [[CrossRef](#)]
124. Qu, Z.; Na, W.; Liu, X.; Liu, H.; Su, X. A novel fluorescence biosensor for sensitivity detection of tyrosinase. *Anal. Chim. Acta* **2018**, *997*, 52–59. [[CrossRef](#)] [[PubMed](#)]
125. Cui, F.; Ji, J.; Sun, J.; Wang, J.; Zhang, Y.; Ding, H.; Lu, Y.; Xu, D.; Sun, X. A novel magnetic fluorescent biosensor based on graphene quantum dots for rapid, efficient, and sensitive separation and detection of circulating tumor cells. *Anal. Bioanal. Chem.* **2019**, *411*, 985–995. [[CrossRef](#)] [[PubMed](#)]
126. Lv, Y.-K.; Li, Y.-Y.; Yao, H.-C.; Li, Z.-J. Nitrogen-doped graphene quantum dots-modified mesoporous SnO<sub>2</sub> hierarchical hollow cubes for low temperature detection of nitrogen dioxide. *Actuators B* **2021**, *339*, 129882. [[CrossRef](#)]
127. Hakimi, M.; Salehi, A.; Boroumand, F.A.; Mosleh, N. Fabrication of a Room Temperature Ammonia Gas Sensor Based on Polyaniline with N-doped Graphene Quantum Dots. *IEEE Sens. J.* **2018**, *18*, 2245–2252. [[CrossRef](#)]

128. Parvizi, R.; Azad, S.; Dashtian, K.; Ghaedi, M.; Heidari, H. Natural Source-Based Graphene as Sensitising Agents for Air Quality Monitoring. *Sci. Rep.* **2019**, *9*, 3798. [[CrossRef](#)]
129. Liu, W.; Zhou, X.; Xu, L.; Zhu, S.; Yang, S.; Chen, X.; Dong, B.; Bai, X.; Lu, G.; Song, H. Graphene quantum dot-functionalized three-dimensional ordered mesoporous ZnO for acetone detection toward diagnosis of diabetes. *Nanoscale* **2019**, *11*, 11496–11504. [[CrossRef](#)]
130. Arunragas, S.; Seekaew, Y.; Pon-On, W.; Wongchoosuk, C. Hydroxyl edge-functionalized Graphene quantum dots for gas-sensing applications. *Diam. Relat. Mater.* **2020**, *105*, 107790. [[CrossRef](#)]
131. Gavgani, J.N.; Hasani, A.; Nouri, M.; Mahyarii, M.; Salehii, A. Highly sensitive and flexible ammonia sensor based on S and N co-doped graphene quantum dots/polyaniline hybrid at room temperature. *Sens. Actuators B* **2016**, *229*, 239–248. [[CrossRef](#)]
132. Hakimi, M.; Salehi, A.; Boroumand, F. Fabrication and Characterization of an Ammonia Gas Sensor Based on PEDOT-PSS with N-doped Graphene Quantum Dots Dopant. *IEEE Sens. J.* **2016**, *16*, 6149–6154. [[CrossRef](#)]
133. Abbasabadi, M.K.; Zand, H.R.E.; Khodabakhshi, S.; Gholami, P.; Rashidi, A. Synthesis of new functionalized reduced graphene oxide quantum dot composite for high-performance NO<sub>2</sub> gas sensor. *Res. Chem. Intermed.* **2021**, *47*, 2279–2296. [[CrossRef](#)]
134. Lv, Y.; Li, Y.; Zhou, R.-H.; Pan, Y.-P.; Yao, H.-C.; Li, Z. N-Doped graphene quantum dots-decorated three-dimensional ordered macroporous In<sub>2</sub>O<sub>3</sub> for NO<sub>2</sub> sensing at low temperatures. *ACS Appl. Mater. Interfaces* **2020**, *12*, 34245–34253. [[CrossRef](#)] [[PubMed](#)]
135. Xue, B.; Yang, Y.; Tang, R.; Sun, Y.; Sun, S.; Cao, X.; Li, P.; Zhang, Z.; Li, X. One-step hydrothermal synthesis of a flexible nanopaper-based Fe<sup>3+</sup> sensor using carbon quantum dot grafted cellulose nanofibrils. *Cellulose* **2020**, *27*, 729–742. [[CrossRef](#)]
136. Shi, L.; Li, Y.; Li, X.; Zhao, B.; Wen, X.; Zhang, G.; Dong, C.; Shuang, S. Controllable synthesis of green and blue fluorescent carbon nanodots for pH and Cu<sup>(2+)</sup> sensing in living cells. *Biosens. Bioelectron.* **2016**, *77*, 598–602. [[CrossRef](#)] [[PubMed](#)]
137. Xu, H.; Zhang, K.; Liu, Q.; Liu, Y.; Xie, M. Visual and fluorescent detection of mercury ions by using a dually emissive ratiometric nanohybrid containing carbon dots and CdTe quantum dots. *Microchim. Acta* **2017**, *184*, 1199–1206. [[CrossRef](#)]
138. Das, R.; Sugimoto, H.; Fujii, M.; Giri, P.K. Quantitative understanding of charge-transfer-mediated Fe<sup>3+</sup> sensing and fast photoresponse by N-doped graphene quantum dots decorated on plasmonic Au nanoparticles. *ACS Appl. Mater. Interfaces* **2020**, *12*, 4755–4768. [[CrossRef](#)]
139. Li, M.; Chen, T.; Gooding, J.J.; Liu, J. Review of carbon and graphene quantum dots for sensing. *ACS Sens.* **2019**, *4*, 1732–1748. [[CrossRef](#)]
140. Wang, C.; Tao, H.; Cheng, L.; Liu, Z. Near-infrared light induced in vivo photodynamic therapy of cancer based on upconversion nanoparticles. *Biomaterials* **2011**, *32*, 6145–6154. [[CrossRef](#)]
141. Gao, X.; Cui, Y.; Levenson, R.M.; Chung, L.W.K.; Nie, S. In vivo cancer targeting and imaging with semiconductor quantum dots. *Nat. Biotechnol.* **2004**, *22*, 969–976. [[CrossRef](#)]
142. Ju, J.; Regmi, S.; Fu, A.; Lim, S.; Liu, Q. Graphene quantum dot based chargereversal nanomaterial for nucleus-targeted drug delivery and efficiency controllable photodynamic therapy. *Biophotonics* **2019**, *12*, e201800367. [[CrossRef](#)] [[PubMed](#)]
143. Li, J.-L.; Tang, B.; Yuan, B.; Sun, L.; Wang, X.-G. A review of optical imaging and therapy using nanosized graphene and graphene oxide. *Biomaterials* **2013**, *34*, 9519–9534. [[CrossRef](#)]
144. Cao, Y.; Dong, H.; Yang, Z.; Zhong, X.; Chen, Y.; Dai, W.; Zhang, X. Aptamer-conjugated graphenequantum dots/porphyrin derivative theranostic agent for intracellular cancer-related microRNA detection and fluorescence-guided photothermal/photodynamic synergetic therapy. *ACS Appl. Mater. Interfaces* **2017**, *9*, 159–166. [[CrossRef](#)] [[PubMed](#)]
145. Yao, X.; Tian, Z.; Liu, J.; Zhu, Y.; Hanagata, N. Mesoporous silica nanoparticles capped with graphene quantum dots for potential chemo-photothermal synergistic cancer therapy. *Langmuir* **2017**, *33*, 591–599. [[CrossRef](#)] [[PubMed](#)]
146. Jin, K.; Gao, H.; Lai, L.; Pang, Y.; Zheng, S.; Niu, Y.; Li, X. Preparation of highly fluorescent sulfur doped graphene quantum dots for live cell imaging. *J. Lumin.* **2018**, *197*, 147–152. [[CrossRef](#)]
147. Kuo, W.-S.; Shen, X.-C.; Chang, C.-Y.; Kao, H.-F.; Lin, S.-H.; Wang, J.-Y.; Wu, P.-C. Multiplexed graphene quantum dots with excitation-wavelength-independent photoluminescence, as two-photon probes, and in ultraviolet-near Infrared bioimaging. *ACS Nano* **2020**, *14*, 11502–11509. [[CrossRef](#)]
148. Li, G.; Liu, Z.; Gao, W.; Tang, B. Recent advancement in graphene quantum dots based fluorescent sensor: Design, construction and bio-medical applications. *Coord. Chem. Rev.* **2023**, *478*, 214966. [[CrossRef](#)]
149. Zhao, X.-E.; Lei, C.; Gao, Y.; Gao, H.; Zhu, S.; Yang, X.; You, J.; Wang, H. A ratiometric fluorescent nanosensor for the detection of silver ions using graphene quantum dots. *Sens. Actuators B Chem.* **2017**, *253*, 239–246. [[CrossRef](#)]
150. Liu, Z.; Mo, Z.; Niu, X.; Yang, X.; Jiang, Y.; Zhao, P.; Liu, N.; Guo, R. Highly sensitive fluorescence sensor for mercury(II) based on boron- and nitrogen-co-doped graphene quantum dots. *J. Colloid Interface Sci.* **2020**, *566*, 357–368. [[CrossRef](#)]
151. Xu, A.; He, P.; Ye, C.; Liu, Z.; Gu, B.; Gao, B.; Li, Y.; Dong, H.; Chen, D.; Wang, G.; et al. Polarizing graphene quantum dots toward long-acting intracellular reactive oxygen species evaluation and tumor detection. *ACS Appl. Mater. Interfaces* **2020**, *12*, 10781–10790. [[CrossRef](#)] [[PubMed](#)]
152. Liang, B.; Zhao, D.; Liu, Y.; Guo, X.; Zhang, H.; Zhang, L.; Zheng, C. Chemoembolization of liver cancer with doxorubicin-loaded CalliSpheres microspheres: Plasma pharmacokinetics, intratumoral drug concentration, and tumor necrosis in a rabbit model. *Drug Deliv. Transl. Res.* **2020**, *10*, 185–191. [[CrossRef](#)] [[PubMed](#)]
153. Shi, J.; Votruba, A.R.; Farokhzad, O.C.; Langer, R. Nanotechnology in drug delivery and tissue engineering: From discovery to applications. *Nano Lett.* **2010**, *10*, 3223–3230. [[CrossRef](#)] [[PubMed](#)]

154. Tasciotti, E.; Liu, X.; Bhavane, R.; Plant, K.; Leonard, A.D.; Price, B.K.; Cheng, M.M.-C.; Decuzzi, P.; Tour, J.M.; Robertson, F.; et al. Mesoporous silicon particles as a multistage delivery system for imaging and therapeutic applications. *Nat. Nanotechnol.* **2008**, *3*, 151–157. [[CrossRef](#)]
155. Wang, C.; Wu, C.; Zhou, X.; Han, T.; Xin, X.; Wu, J.; Zhang, J.; Guo, S. Enhancing cell nucleus accumulation and DNA cleavage activity of anti-cancer drug via graphene quantum dots. *Sci. Rep.* **2013**, *3*, 2852. [[CrossRef](#)]
156. Iannazzo, D.; Pistone, A.; Salamò, M.; Galvagno, S.; Romeo, R.; Giofrè, S.V.; Branca, C.; Visalli, G.; Di Pietro, A. Graphene quantum dots for cancer targeted drug delivery. *Int. J. Pharm.* **2017**, *518*, 185–192. [[CrossRef](#)]
157. Sung, S.-Y.; Su, Y.-L.; Cheng, W.; Hu, P.-F.; Chiang, C.-S.; Chen, W.-T.; Hu, S.-H. Graphene quantum dots-mediated theranostic penetrative delivery of drug and photolytics in deep tumors by targeted biomimetic nanosponges. *Nano Lett.* **2019**, *19*, 69–81. [[CrossRef](#)]

**Disclaimer/Publisher’s Note:** The statements, opinions and data contained in all publications are solely those of the individual author(s) and contributor(s) and not of MDPI and/or the editor(s). MDPI and/or the editor(s) disclaim responsibility for any injury to people or property resulting from any ideas, methods, instructions or products referred to in the content.